



VICTORIA UNIVERSITY
MELBOURNE AUSTRALIA

Comparison of protection against mpox following mRNA or modified vaccinia Ankara vaccination in nonhuman primates

This is the Published version of the following publication

Mucker, Eric M, Freyn, Alec W, Bixler, Sandra L, Cizmeci, Deniz, Atyeo, Caroline, Earl, Patricia L, Natarajan, Harini, Santos, Genisis, Frey, Tiffany R, Levin, Rafael H, Meni, Anusha, Asthagiri-Arunkumar, Guha A, Stadlbauer, Daniel, Jorquera, Patricia A, Bennett, Hamilton, Johnson, Joshua, Hardcastle, Kath, Americo, Jeffrey L, Cotter, Catherine A, Koehler, Jeff W, Davis, Christopher I, Shamblin, Joshua, Ostrowski, Kristin, Raymond, Jo L, Ricks, Keersten M, Carfi, Andrea, Yu, WenHan, Sullivan, Nancy J, Moss, Bernard, Alter, Galit and Hooper, Jay W (2024) Comparison of protection against mpox following mRNA or modified vaccinia Ankara vaccination in nonhuman primates. *Cell*, 187 (20). pp. 5540-5553. ISSN 0092-8674

The publisher's official version can be found at

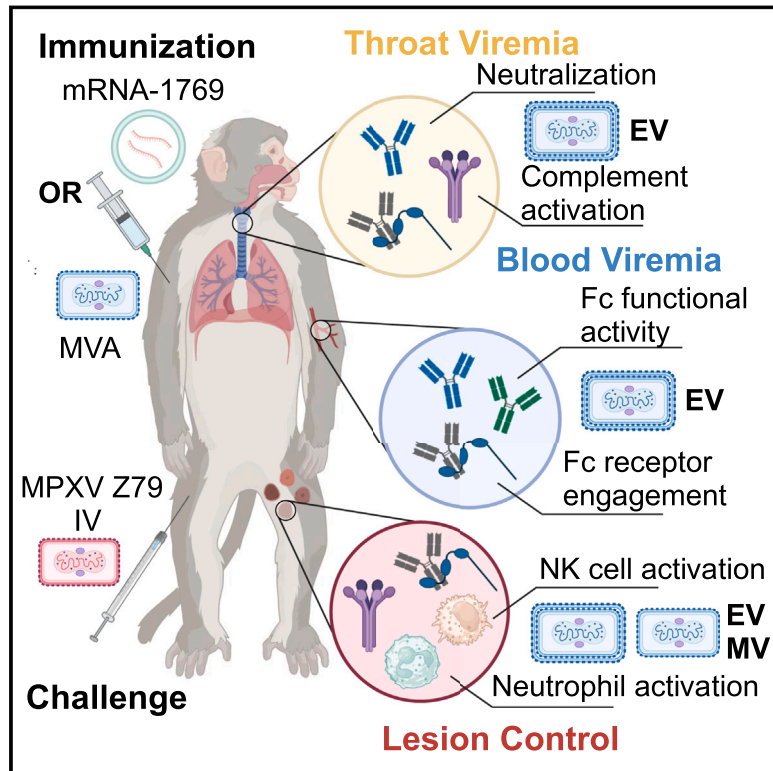
<https://doi.org/10.1016/j.cell.2024.08.043>

Note that access to this version may require subscription.

Downloaded from VU Research Repository <https://vuir.vu.edu.au/49139/>

Comparison of protection against mpox following mRNA or modified vaccinia Ankara vaccination in nonhuman primates

Graphical abstract



Authors

Eric M. Mucker, Alec W. Freyn, Sandra L. Bixler, ..., Bernard Moss, Galit Alter, Jay W. Hooper

Correspondence

galit.alter@modernatx.com (G.A.), jay.w.hooper.civ@health.mil (J.W.H.)

In brief

An mRNA vaccine was designed against Orthopoxviruses (including mpox and smallpox) and compared with current standard of care modified vaccinia Ankara (MVA) vaccines in a nonhuman primate model of lethal mpox virus infection. In-depth immunological profiling revealed a critical role for Fab and Fc functions against aspects of poxvirus disease and provided broad pan-Orthopoxvirus immunity.

Highlights

- mRNA-1769 resulted in lower lesions and reduced viral replication compared with MVA
- mRNA-1769 induced enhanced neutralizing and functional antibodies compared with MVA
- Both Fab- and Fc-receptor-binding antibodies were associated with viral control
- MV and EV antibodies correlated with viremia and lesional control, respectively



Short article

Comparison of protection against mpox following mRNA or modified vaccinia Ankara vaccination in nonhuman primates

Eric M. Mucker,^{1,8} Alec W. Freyn,^{2,8} Sandra L. Bixler,^{1,8} Deniz Cizmeci,² Caroline Atyeo,² Patricia L. Earl,³ Harini Natarajan,² Genesis Santos,² Tiffany R. Frey,² Rafael H. Levin,² Anusha Meni,² Guha A. Arunkumar,² Daniel Stadlbauer,² Patricia A. Jorquera,² Hamilton Bennett,² Joshua C. Johnson,² Kath Hardcastle,² Jeffrey L. Americo,³ Catherine A. Cotter,³ Jeff W. Koehler,¹ Christopher I. Davis,¹ Joshua D. Shamblin,¹ Kristin Ostrowski,¹ Jo Lynne Raymond,¹ Keersten M. Ricks,¹ Andrea Carfi,² Wen-Han Yu,² Nancy J. Sullivan,^{4,5,6} Bernard Moss,³ Galit Alter,^{2,7,*} and Jay W. Hooper^{1,7,9,*}

¹Virology Division, United States Army Medical Research Institute of Infectious Diseases, Fort Detrick, MD, USA

²Moderna Inc., Cambridge, MA, USA

³Laboratory of Viral Diseases, National Institute of Allergy and Infectious Diseases, National Institutes of Health, Bethesda, MD, USA

⁴National Emerging Infectious Diseases Laboratories (NEIDL), Boston University, Boston, MA, USA

⁵Department of Virology, Immunology, and Microbiology, Boston University School of Medicine, Boston, MA, USA

⁶Department of Biology, Boston University, Boston, MA, USA

⁷Senior author

⁸These authors contributed equally

⁹Lead contact

*Correspondence: galit.alter@modernatx.com (G.A.), jay.w.hooper.civ@health.mil (J.W.H.)

<https://doi.org/10.1016/j.cell.2024.08.043>

SUMMARY

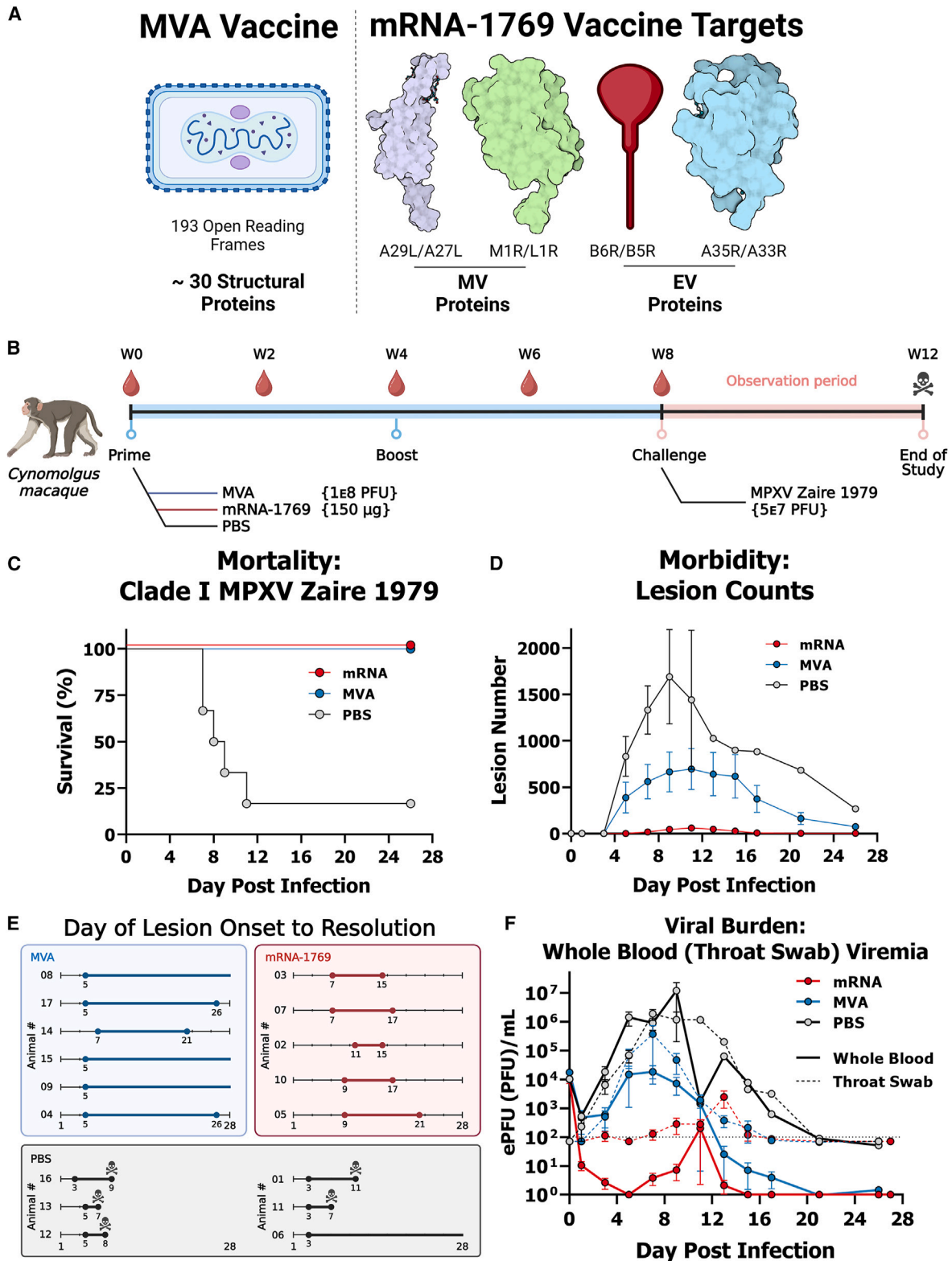
In 2022, mpox virus (MPXV) spread worldwide, causing 99,581 mpox cases in 121 countries. Modified vaccinia Ankara (MVA) vaccine use reduced disease in at-risk populations but failed to deliver complete protection. Lag in manufacturing and distribution of MVA resulted in additional MPXV spread, with 12,000 reported cases in 2023 and an additional outbreak in Central Africa of clade I virus. These outbreaks highlight the threat of zoonotic spillover by Orthopoxviruses. mRNA-1769, an mRNA-lipid nanoparticle (LNP) vaccine expressing MPXV surface proteins, was tested in a lethal MPXV primate model. Similar to MVA, mRNA-1769 conferred protection against challenge and further mitigated symptoms and disease duration. Antibody profiling revealed a collaborative role between neutralizing and Fc-functional extracellular virion (EV)-specific antibodies in viral restriction and opsonophagocytic and cytotoxic antibody functions in protection against lesions. mRNA-1769 enhanced viral control and disease attenuation compared with MVA, highlighting the potential for mRNA vaccines to mitigate future pandemic threats.

INTRODUCTION

Mpox virus (MPXV) is a zoonotic virus from the genus Orthopoxvirus, which also includes variola virus (VARV), the causative agent of smallpox disease estimated to have had a 30% mortality rate prior to its eradication in 1980.¹ The first human infection with MPXV was identified in 1970 in the Democratic Republic of Congo (DRC),² and this virus species can be divided into two clades: a virulent clade I strain causing approximately 10% lethality and a second clade II strain associated with roughly <1%–3% mortality depending on the outbreak and strain.³ Since its discovery, MPXV has been linked to repeated small-scale endemic outbreaks in Western and Central Africa. However, these outbreaks have increased in frequency over the past decades, likely in the wake of declining population-level immunity

to smallpox.⁴ Moreover, in the summer of 2022, a clade II strain of MPXV spilled out of traditional endemic regions and spread globally, causing over 90,000 mpox cases and 170 deaths.⁵ Mitigation of viral spread occurred primarily through social countermeasures such as education and community engagement to mitigate spread as well as the use of therapeutic drugs (e.g., tecovirimat) and a contemporary modified vaccinia Ankara (MVA)-based vaccine (JYNNEOS), which offered 35% to 75% protection after a single dose and 66% to 85% protection after two doses in real-world studies.^{6–9} Additionally, an outbreak of clade I virus began in the DRC in 2023 and has spread through Central Africa, causing substantial mortality, with more than 500 deaths reported in August 2024 at a fatality rate of around 2.9%.¹⁰ Despite the effectiveness of the JYNNEOS vaccine against mpox, issues in supply,¹¹ unfavorable reactogenicity,¹¹





(legend on next page)

incomplete immunity,¹¹ and uncertainty of cross-protection to more virulent strains provide critical motivation for the development of a potential new vaccine modality for improved vaccines to cover these gaps.^{8,11}

Among the emerging vaccine platforms, mRNA vaccines offer unprecedented flexibility, speed, and immunogenicity.^{12,13} Yet, whether an mRNA vaccine could offer comparable immune protection to a whole attenuated poxviral vaccine vector remained unclear. Four well-defined Orthopoxvirus protein targets were defined following deep immune profiling of protective vaccinia virus (VACV)-induced immune responses.^{14,15} Two of the selected antigens are present on extracellular virions (EVs) and two are found on the mature virion (MV) surface, all of which are involved in viral attachment and infection and have been demonstrated to confer protection when delivered as protein or DNA vaccines to murine, rabbit, and macaque models.^{14,15} While limited protection was achieved by individual antigens, the combination of the four antigens, A29, A35, B6, and M1, provided optimal protection^{16,17} and protected nonhuman primates (NHPs) against intravenous (IV) MPXV challenge.¹⁸ Moreover, monoclonal antibodies to these targets provided protection in mice, and depletion of B cells, but not CD4+ or CD8+ T cells, abrogated protection, highlighting the key role of humoral immune response to protection.^{18,19} Along these lines, mRNA vaccination with the same four key MPXV EV/MV antigens resulted in protection against heterologous VACV infection, linked to robust neutralizing and Fc-effector functions.²⁰ However, whether an mRNA vaccine could provide protection against a lethal MPXV virus as well as attenuate disease remained unclear.

Here, we utilized a stringent clade I MPXV Zaire 1979 (Z79) MPXV NHP challenge model to assess the protective efficacy of an mRNA-lipid nanoparticle (LNP) vaccine, mRNA-1769, expressing optimized versions of the four MPXV antigens of interest (A29, A35, B6, and M1) compared with MVA.^{20,21} Clinically relevant doses were utilized for the administration of both the mRNA and MVA vaccines. While both MVA and mRNA-1769 conferred complete protection following lethal MPXV challenge, mRNA-immunized animals experienced 10-fold fewer lesions, reduced duration of disease, and substantial mitigation of circulating and mucosal viremia in the mRNA cohort. Deep immunological profiling of the humoral response through classical binding and neutralization assays as well as systems serology approaches revealed more robust MPXV neutralizing responses, broadly reactive heterologous neutralizing titers, and greater functional humoral immune responses against the four MPXV

antigens in mRNA-1769 immunized animals compared with MVA-immunized NHPs. Additionally, immune correlates analyses highlighted the critical coordination between both neutralizing and Fc-effector functions against both EV and MV targets, EV-Fc target-specific functions and neutralization as key correlates of antiviral control, and EV target-antigen-specific opsonophagocytic activity and neutrophil/natural killer (NK) cell-targeted functions to the MV as key determinants of lesion control. These findings suggest that an mRNA-LNP vaccine expressing four key MPXV proteins induces a robust functional humoral response that protects against a lethal MPXV challenge similarly to MVA immunization but confers superior protection against disease, implying that there is room for improvement in the contemporary vaccine arsenal aimed at protecting from emerging Orthopoxviral threats.

RESULTS

Efficacy of mRNA-based and MVA vaccines in a lethal NHP mpox virus infection model

The rapid deployment of the MVA-based vaccine (JYNNEOS) during the unprecedented 2022 global mpox outbreak provided rapid protection to at-risk populations.^{7,22} While the vaccine reduced spread and lessened the burden of disease, vaccine production and incomplete protective immunity¹¹ highlighted the potential need for next-generation vaccine development. Unlike the replication-deficient JYNNEOS vaccine, which expresses all viral antigens, protein- and nucleic-acid-based vaccines focus on a subset of viral surface antigens expressed on the MV and the EV that are highly conserved across all old-world Orthopoxviruses.²³ Importantly, the combination of four specific antigens was essential to achieve full protection,²⁴ and mRNA-based expression of these four antigens (MV: A29 and M1; EV: B6 and A35; Figure 1A) resulted in near sterilizing protection against a heterologous lethal VACV challenge.²⁰ However, whether this vaccine could confer protection against a lethal MPXV challenge in a primate model and modify disease compared with MVA remained incompletely defined.

The protective efficacy and disease-modulating activity of an mRNA-LNP MPXV vaccine, mRNA-1769, was therefore tested compared with a live attenuated Orthopoxvirus vaccine (MVA) in cynomolgus macaques following a lethal challenge with MPXV clade I Z79. Animals were randomized into 3 groups of 6 animals each and immunized with 150 μ g of mRNA-1769, 100 M plaque-forming units (PFUs) of MVA or were administered a saline control (PBS) in a prime boost fashion with 4 weeks

Figure 1. mRNA vaccination induces superior protection from lethal MPXV challenge in an NHP model

(A) Illustration of the differences in vaccines used for this study. Modified vaccinia Ankara (MVA) is a live attenuated virus, while mRNA-1769 contains four mRNA molecules that each express an Orthopoxvirus surface protein. PDB models 3VOP, 1YPY, and 3K7B were used to represent the antigens of interest.

(B) Study design of NHP immunization and challenge periods in weeks (W), immunizations were performed intramuscularly, and challenge was performed intravenously ($n = 6$ /group).

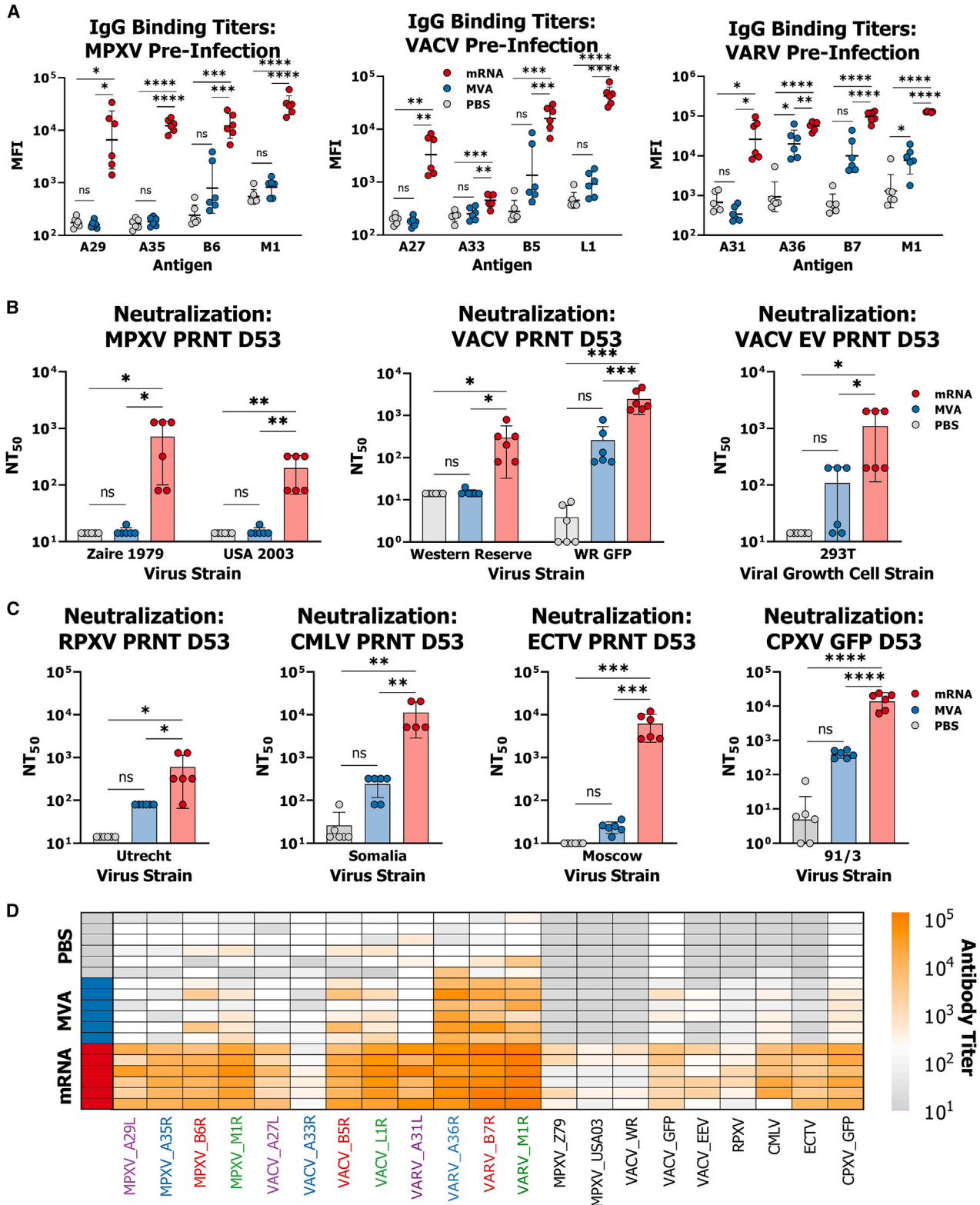
(C) Survival percentages of each group during the challenge period ($n = 5$ – 6 /group).

(D) Number of MPXV lesions per animal is shown for each group as the average \pm standard error of the mean ([SEM]; $n = 5$ – 6 /group).

(E) Duration of mpox disease is shown for each individual animal during the challenge period, with the day of lesion appearance and resolution noted. Date of euthanasia is noted with a skull symbol.

(F) Genome counts (estimated plaque-forming units [PFUs]) per mL of whole blood were collected by quantitative PCR, and PFU of throat swabs was assessed by plaque assay from samples acquired during the challenge period. The average \pm SEM is reported for each group ($n = 5$ – 6 /group).

See also Figure S1.



(legend on next page)

between immunizations (Figure 1B). Given that the mucosal challenge route exhibits a delayed progression to lesional severe disease and provides a lower bar of protection, here we elected to perform an IV challenge that mimics similar viral burst dynamics as those observed in humans.^{25,26} Moreover, the more faithful disease pathology observed with IV challenge enabled a more rigorous ability to compare protection afforded by mRNA in contrast to MVA for the first time. Thus, serum was collected from animals every 2 weeks prior to IV challenge with 50 M PFUs of MPXV Z79. Animals were observed daily for signs of disease progression and lesion counts. Throat swabs and whole blood were taken every other day during the period of infection. Animals reaching predetermined viability criteria prior to the end of the study were humanely euthanized. One animal in the mRNA-immunized group did not recover from an anesthesia event prior to challenge and was not included in the challenge portion of the study.

Animals receiving MVA and mRNA-1679 were completely protected from lethality of MPXV Z79 infection, while five out of six NHPs in the PBS group succumbed to infection (Figure 1C). Body weight was tracked from the time of challenge, marked by significant weight loss in the PBS group, maintenance of weight in the MVA-immunized animals, and increasing weight in the mRNA arm (Figure S1A). MPXV lesion numbers were used as a critical metric of disease burden and morbidity, increasing substantially in the PBS group during the course of infection with a peak average lesion count of 1,448 (Figure 1D). MVA-immunized animals experienced reduced lesion counts relative control animals with an average maximum lesion count of 607 for the group. By contrast, mRNA-immunized animals showed the fewest lesions per NHP across the duration of infection with a peak average lesion count of 54. Given that the World Health Organization (WHO) classifies severe disease as greater than 100 lesions and grave disease as greater than 250 lesions per individual, all PBS control animals experience grave disease, and four out of six animals in the MVA group displayed grave disease, with all other animals exhibiting severe disease (Figure S1C). By contrast, all animals in the mRNA-immunized group did not reach the criteria for severe disease.

The duration of disease was also measured as a function of lesion onset to resolution and charted for each individual animal (Figure 1E). The duration of disease was reduced by over 10 days when comparing MVA-immunized animals to those receiving the mRNA vaccine (Figure S1B). Additionally, viral burden during the course of infection was determined via the assessment of plaque assay of throat swabs for direct infectious virus measurement

(Figure 1F) and whole blood viremia by quantitative polymerase chain reaction (qPCR; see Figure S1D). Control animals showed substantial viral burden with a peak viral load at day 11 post infection in blood viremia with reduced viral loads in the surviving animals until the end of the study period. MVA-immunized animals exhibited reduced viral loads in blood viremia and infectious virus in the throat compared with PBS-treated animals; however, viral loads in MVA-immunized animals increased until day 7 post infection after which viral loads in the blood and the throat declined until 3 weeks post infection. NHPs receiving mRNA-1769 vaccine exhibited superior control of infection in both the blood and the throat with a slight rebound on day 11 in the blood and day 13 in the throat before rapid control. Thus, collectively, while both MVA and mRNA-1769 provided robust protection against lethal MPXV challenge, mRNA-1769 provided superior protection against weight loss, lesion numbers, lesion duration, and viral replication in the throat and the blood.

Distinct binding and neutralizing antibody responses across vaccine modalities

To begin to define immunologic differences across the two vaccine platforms that could explain differences in disease burden, we next profiled the humoral immune response across the animal groups at peak immunogenicity 2 weeks after the boost. Binding antibodies were first analyzed to antigens representative of those included in mRNA-1769 derived from the contemporary 2022 strain of MPXV clade II, MVA, or the India 1967 strain of VARV (Figures 2A, S2A, and S2B). For all antigens tested, antibody responses were significantly higher in the mRNA group than the MVA and PBS groups. Two NHPs in the MVA group elicited detectable antibody responses against both MPXV B6 and VACV B5. MVA-immunized animals did elicit anti-VARV antigen responses for A33, B5, and L1 that were above the background set by control immunized animals. Additionally, antibody responses against a lysed whole-virus preparation of MVA were tested by enzyme-linked immunosorbent assay (ELISA) to determine the overall virion binding titers (Figures S2C and S2D). Despite the exposure of MVA-immunized animals to the whole matched virus, binding titers remained significantly highest in mRNA-1769 immunized animals to lysed whole-virus.

To further assay the functional potential of vaccine-induced antibodies, we next performed neutralizing antibody assays utilizing serum immediately prior to challenge (Figure 2B). Plaque reduction neutralization tests (PRNTs) were performed against MPXV strains clade I Z79 and clade II USA 2003 (Figures 2B, left, and S2E) and the VACV strain Western Reserve

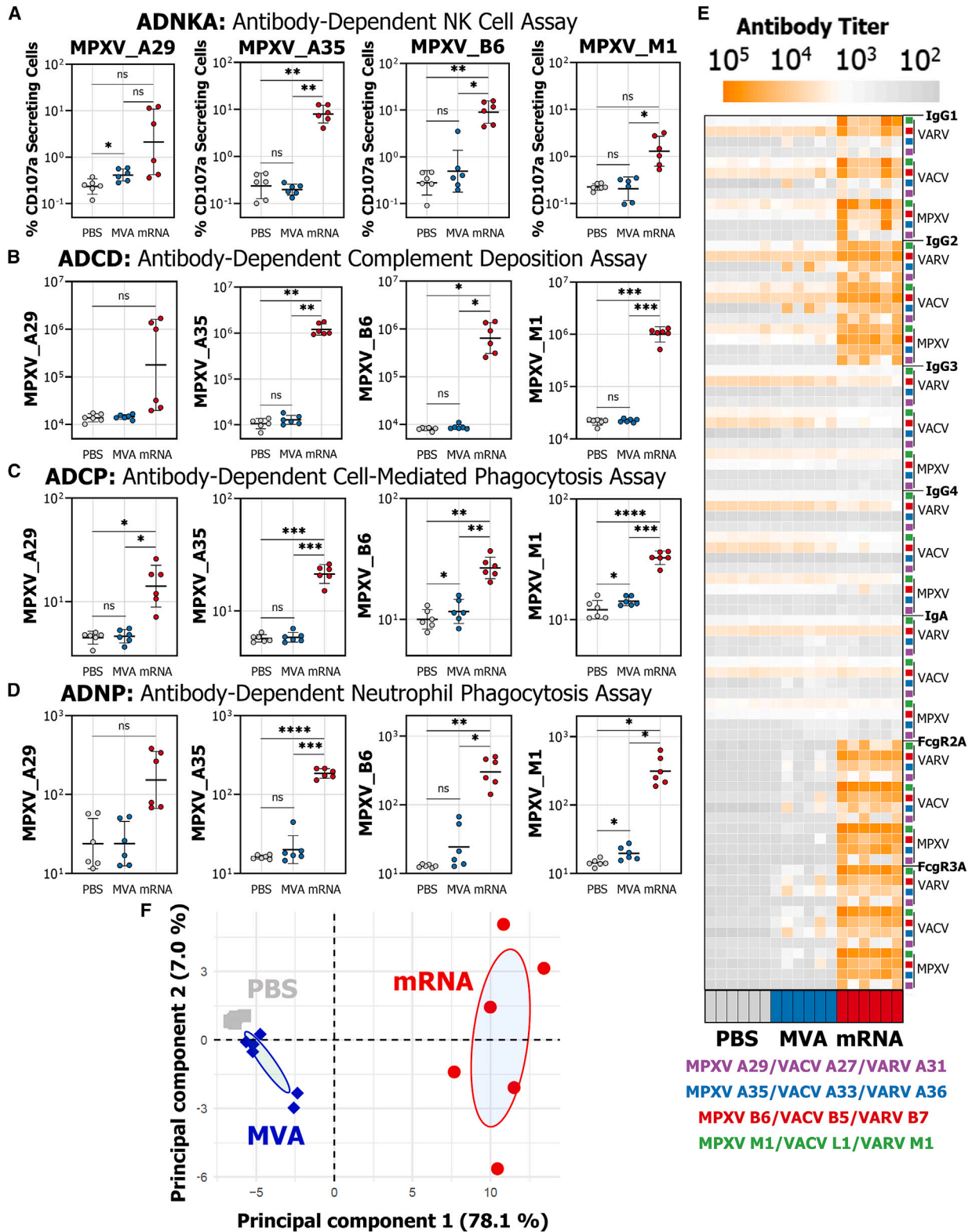
Figure 2. Immunization with MPXV antigen-encoding mRNA-LNP vaccine drives a robust and broad humoral response

(A) IgG binding titers against antigens derived from MPXV, VACV, or VARV were assessed at day 40 post-prime. Data are shown as the average median fluorescence intensity per sample ran in duplicate. Crossbars represent the geometric mean of the group \pm geometric standard deviation ($n = 6/\text{group}$).

(B and C) Fifty percent neutralization titers are shown for each individual animal ran in singlet or duplicate using the plaque reduction neutralization test. For VACV and CPXV strains expressing GFP, the reduction in the number of GFP fluorescent cells was utilized rather than reduction in viral plaques. VACV EV neutralization was performed in the presence of an anti-MV monoclonal antibody to assess only EV-specific responses. Bars represent the average \pm SD per group ($n = 6/\text{group}$).

(D) A heatmap of all antibody binding and neutralization data is shown for each individual animal. Values were background corrected by subtracting the average of pre-immunization responses for each analyte. Statistical testing was performed using a one-way ANOVA with Tukey's correction for multiple comparisons ($^*p < 0.05$, $^{**}p < 0.01$, $^{***}p < 0.001$, and $^{****}p < 0.0001$).

See also Figure S2.



(legend on next page)

(WR; Figure 2B, middle), which was also tested as a high-throughput green fluorescence protein (GFP)-expressing VACV to compare to the traditional PRNT assay. A PRNT assay performed in the presence of complement and monoclonal antibodies to remove MV was also performed to assess the contribution of EV-specific antibody responses to neutralization (Figure 2B, right). mRNA-immunized NHPs elicited robust neutralizing titers, which were significantly higher than those elicited by MVA or PBS inoculation for any virus tested. MVA immunization did not elicit neutralizing antibody responses to either MPXV tested, except for one animal, which was slightly above the limit of detection. Similar results were seen for the PRNT assay with VACV WR, though the GFP-expressing version of this virus did detect VACV-neutralizing responses above background but not statistically significantly greater than the PBS-immunized response. EV-specific neutralizing responses were seen after MVA immunization in half of the immunized animals, but the overall group did not differ significantly from the PBS group. By contrast, all mRNA-immunized animals induced robust EV-specific neutralizing antibody responses. Kinetics of neutralizing responses demonstrate a moderate neutralizing response after prime with a substantial increase in titers upon boost with mRNA-1769 (Figures S2E–S2G). Additionally, neutralization tests were performed against additional Orthopoxvirus strains to test the breadth of the vaccine-induced immune response (Figure 2C). Rabbitpox, camelpox, and ectromelia viruses were utilized in PRNTs. In addition, a GFP-expressing cowpox virus strain was utilized in a microneutralization assay. Robust neutralizing responses were observed against each heterologous viral strain in animals immunized with mRNA-1769, while those immunized with MVA did not show a statistically significant increase in titers compared with the PBS-immunized NHP for any virus. Moreover, integration of all antibody measurements highlighted a clear gradient of Orthopoxvirus-specific immunity across the 3 groups of animals, with intermediate levels of antibodies largely targeting VACV antigens among MVA-immunized animals and cross-reactive binding titers and neutralizing antibody responses among mRNA-immunized macaques (Figure 2D). These data point to the induction of robust, broadly cross-reactive humoral immune responses in mRNA-1769-immunized animals that may explain differential antiviral control across the groups and the potential to protect across a wide range of Orthopoxviruses.

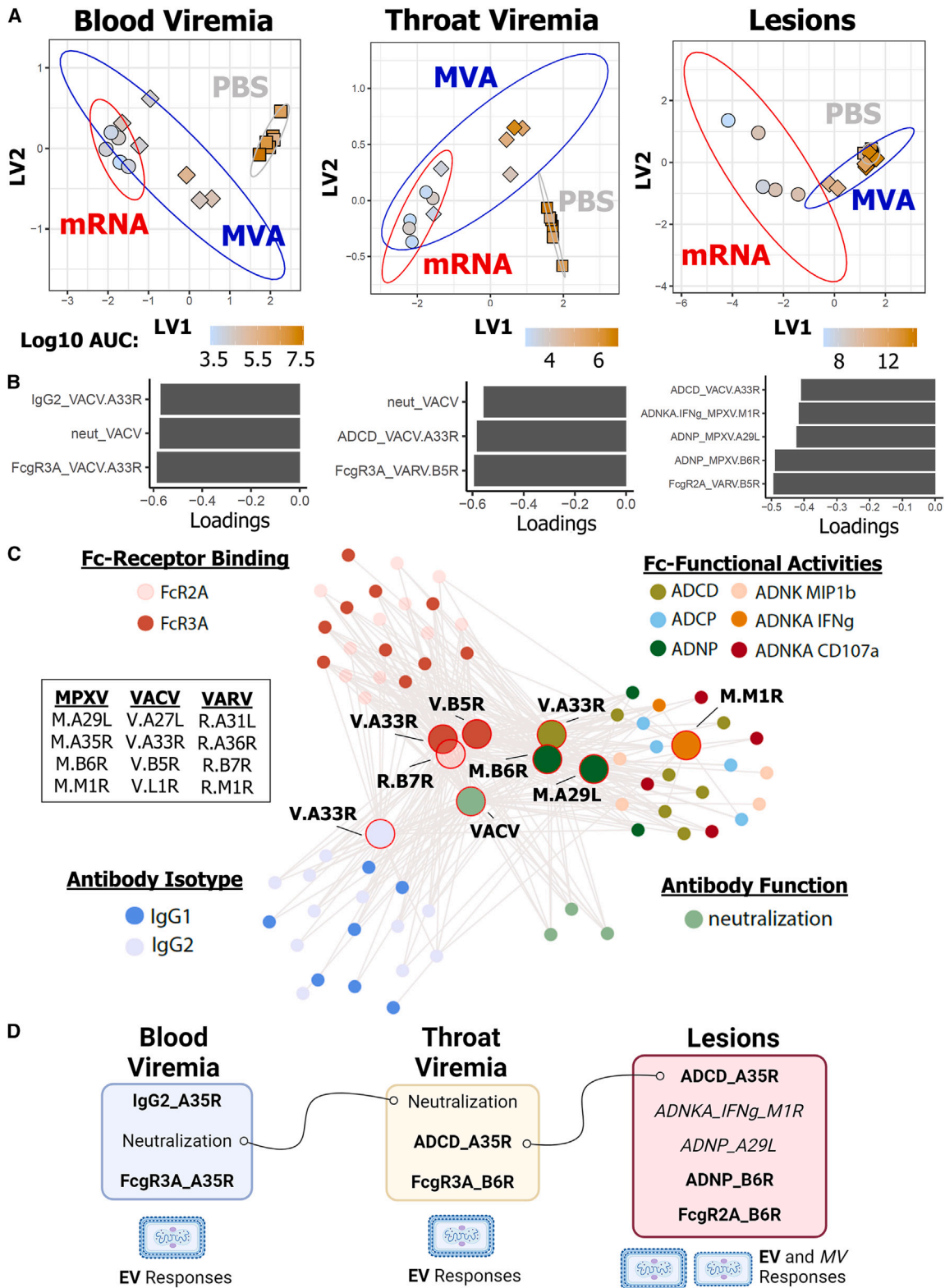
Antibody Fc-effector profiles differ across vaccine modalities

Beyond the role of neutralizing antibodies in antiviral protection against poxviruses, additional antibody functions, including antibody-mediated complement activation,²⁷ have been implicated in protection. Thus, despite the low-level neutralization induced by MVA, we next profiled humoral immune responses across all 3 groups at peak immunogenicity using systems serology (Figures 3A–3D). NK cell activation (ADNK) was observed across the mRNA-immunized animals, although limited to no ADNK activity was observed across the 4 antigens in the PBS and MVA-immunized animals (Figure 3A). Detectable NK cell degranulation, interferon- γ (IFN γ) release, and macrophage inflammatory protein-1 (MIP1b) to the A35, B6, and M1 antigens were observed in mRNA-immunized animals, with dichotomized ADNK activity to the A29 antigen (Figures S3A–S3D). While limited antibody-dependent complement deposition (ADCD) was observed in the PBS and MVA-immunized animals, ADCD responses were observed with the same kinetics and robust peak immune titers to A35, B6, and M1 antigens in all animals (Figure 3B). Similar to that observed for ADNK, half of the mRNA-immunized animals generated ADCD responses to the A29 antigen. Similarly, robust but slightly delayed kinetics were observed for the antibody-dependent cellular monocyte phagocytic (ADCP) response across all 4 antigens in the mRNA-immunized animals (Figure 3C). Additionally, rapid induction of antibody-dependent neutrophil phagocytosis was observed in the mRNA group but not in the MVA-immunized animals for all 4 antigens (Figure 3D).

To further visualize the heterogeneity of the functional humoral immune response, a heatmap of immunoglobulin G (IgG) subclass responses and Fc-receptor-binding profiles was plotted for each individual animal across the 3 vaccine groups (Figure 3E). Importantly, while no 2 animals had identical antibody profiles, the heatmap illustrates the presence of low-level humoral immune responses in the MVA-immunized animals and stronger subclass and Fc-receptor-binding profiles in mRNA-immunized animals to MPXV, VACV, and VARV antigens. Finally, to gauge the overall multivariate antibody profiles across the groups, we combined all the subclass, isotype, Fc-receptor binding, and functional antibody responses captured by systems serology and performed a principal-component analysis (PCA; Figures 3F and S3E). The data highlight the presence of distinct

Figure 3. Fc-functional antibody activities are driven by mRNA immunization and reflected in systems serology assessment

(A) Antibody-dependent complement deposition (ADCD) assay responses are shown for each antigen tested. Responses at day 40 are shown as the average of duplicates for each individual animal. The crossbar represents the median of each group. Data are also shown over time prior to challenge, with each dot representing the average of each group \pm range of responses ($n = 6/\text{group}$).
 (B and C) Antibody-dependent cellular phagocytosis (ADCP) and neutrophil phagocytosis (ADNP) assays data are shown over time prior to challenge, with each dot representing the average of each group \pm range of responses ($n = 6/\text{group}$).
 (D) Antibody-dependent natural killer activation (ADNK) assay data are reported as the percentage of cells secreting the indicated cytokine after stimulation with the relevant antigen. Responses are shown as the average of duplicates for each individual animal, with the crossbar representing the median of each group ($n = 6/\text{group}$). Statistical testing was performed using a one-way ANOVA with Kruskal-Wallis' correction for multiple comparisons ($*p < 0.05$, $**p < 0.01$, $***p < 0.001$, and $****p < 0.0001$).
 (E) Heatmap of systems serology data was collected in a multiplexed Luminex assay for each antigens/analytes (columns) and individual animals (rows). The average of duplicate median fluorescence intensity values is reported for each condition and each individual animal.
 (F) Principal-component analysis (PCA) was performed using neutralization and systems serology data. Each dot represents the profile of an individual animal. See also Figure S3.



(legend on next page)

antibody profiles across all 3 groups of animals. However, critically, while the PBS controls were more homogeneous (clustering together), variation was observed among the MVA-immunized animals, with two animals splitting from the group. Moreover, the mRNA-immunized animals diverged significantly from the PBS control and MVA-immunized groups but also demonstrated some variability across individual animals. The differences between these animals provide a unique opportunity to mine for immune correlates impacting viral replication or lesion numbers during the course of disease.

Antibody correlates track with antiviral control and prevention of lesions

Previous cellular depletion studies following smallpox vaccination in NHPs prior to challenge highlighted the key role of humoral immunity, and not cellular immunity, in protection against MPXV challenge.¹⁸ Thus, to finally define the precise humoral mechanisms that may account for attenuation of disease, we next performed a multivariate correlates analysis (Figure 4). Specifically, humoral immune profiles of all animals were regressed across blood viral loads, throat viral loads, and lesion numbers to begin to define the vaccine-induced mechanisms of protection against different aspects of disease (Figure 4A). Strikingly, vaccine-induced antibody features were able to robustly separate animals based on their systemic viral loads and disease presentation.

A partial least squares regression (PLSR) was performed following least absolute shrinkage and selection operator (LASSO) to identify features that tracked with systemic viral control (Figure 4B, left). Only 3 of the greater than 4 dozen antibody features that were collected were sufficient to separate viral loads across the animals, including VACV A33-IgG2 titers, VACV-neutralizing antibody titers, and A33-FcγR3a binding levels. These data point to a critical collaborative role for neutralization and EV-specific A33-Fc-receptor-binding activity as key predictors of viral control. Similarly, VACV-neutralizing antibody titers were also associated with lower throat viral loads but in collaboration with A33-complement deposition and B5-VARV-FcγR3a, pointing to a critical role for Fc-mediated activity to both EV antigens (Figure 4B, middle). PLSR separation of vaccine-induced antibody profiles by lesion numbers required 5 of the total vaccine-induced antibody features collected across each animal (Figure 4B, right). Predictive features included the EV VARV B7/MPXV B6 FcγR2a and neutrophil phagocytic (ADNP) response as the top features associated with lower lesion numbers. Additionally, neutrophil opsonophagocytosis to the MV MPXV A29 antigen, NK cell activity to the MPXV MV M1 antigen, and complement activity to the EV VACV A33 anti-

gen were also critical predictors in the model, highlighting the critical role for Fc-effector functions to both EV and MV targets in control from disease manifestation. Furthermore, the PLSR selected features were tightly correlated with additional neutrophil, NK, and complement activating features, with neutralization as secondary co-correlates (significance shown in Figure S4).

To further gain a deeper sense of the functional activity of A33-FcγR3a, a correlation network was generated for all the antibody features, highlighting the coordination between A33-FcγR3a and NK cell activation and neutrophil opsonophagocytosis (Figure 4C). These data suggest that Fc-effector function against both MV and EV virus forms, rather than neutralization, may play a critical role in preventing lesion formation. Thus, collectively, these data suggest that neutralization and EV-Fc mechanisms of action may collaborate to control viral replication following infection, but EV and MV-specific humoral antibody effector functions may be key to reducing lesion formation (Figure 4D).

DISCUSSION

The current 2023–2024 mpox outbreak in the DRC has been linked to more than 20,000 documented infections and over 500 deaths.^{10,28} Coupled with the global 2022 mpox outbreak, there is an urgent need to develop strategies to address this insidious zoonotic disease driving unpredictable epidemics and pandemics. While previously developed vaccines provided protection to at-risk populations, safety, supply chain, and incomplete protection have motivated the development of additional vaccine strategies to mitigate the threat posed by Orthopoxviruses. Recent data have noted mRNA-vaccine-induced protection against lethal MPXV challenge in NHPs.²⁹ Using an IV challenge, which mimics human infection and pathology,^{25,26} here we demonstrate that mRNA is equally protective to an MVA-based immunization against death following a lethal MPXV challenge but also provides superior protection to MVA-based immunization with respect to viral load, weight loss, and lesion control. Moreover, this study shows the evolution of broadly cross-reactive antibodies following mRNA vaccination, building on previous data highlighting the critical role for humoral immune responses in protection against MPXV,¹⁸ and we demonstrate that mRNA-mediated protection against morbidity and disease is mediated by a combination of neutralizing and non-neutralizing antibody functions targeting both antigens on the mature and extracellular viral particles. In light of recent data demonstrating a role for complement in neutralizing antibody-mediated protection against MPXV and data highlighting the critical role for NK cells in MPXV-susceptible CAST mice,^{30,31} these data provide critical insights into mRNA-vaccine-induced correlates of

Figure 4. Neutralization, antibody titers, and functional antibody activities are associated with lower viral loads and lower number of lesions

(A) A supervised multivariate model using LASSO+PLSR was established to identify a minimal set of antibody features associated to whole blood viral loads given the data from binding, neutralizing, and functional humoral antibody assays. The model regressed antibody features against the area under the curve (AUC) for the whole blood qPCR data over time.

(B) A final set of were selected by the model that maximally separated animals based on their blood viremia, throat viremia, or lesion counts.

(C) A correlation network analysis was also performed to identify additional antibody features associated with the down-selected model features. Only correlations with BH-adjusted $p < 0.01$ and absolute $\rho > 0.7$ were visualized.

(D) A model summarizing the correlates identified in this study and how they apply to the different functional symptoms of disease is posited.

See also Figure S4.

immunity against MPXV, which can support licensure, provide mechanistic insights on vaccine performance, support optimized vaccine usage in vulnerable populations, and inspire redesign should novel Orthopoxviral threats emerge requiring antigen addition or alteration.

MVA immunization reduced lesions in challenged NHPs, but the majority of MVA-immunized animals were still classified as experiencing “grave” disease based on WHO lesion number classification.³² By contrast, none of the mRNA-immunized animals reached the criteria for “severe” disease during the course of the infection period. While MVA vaccines have been shown to elicit both humoral and cellular immune responses,^{33,34} previous immune correlates analyses demonstrated that MVA-induced humoral immune responses, rather than cellular immune responses, are necessary and sufficient to mediate protection against MPXV challenge.¹⁸ However, MVA-induced humoral immunity may not be sufficiently robust to fully attenuate disease, as has been observed in recent real-world breakthrough studies.^{35,36} Instead, mRNA vaccination is known to induce robust immunogenicity and may improve responses to Orthopoxvirus targets.^{37,38} Here, we observed robust antibody titers against four key antigens known to afford protection via humoral immune mechanisms.³⁹ Moreover, beyond the neutralizing activity of these vaccine-induced immune responses, mRNA immunization also induced robust Fc-effector functions that collaborated with neutralizing antibody activity to provide protection against viral replication and lesion formation.

Beyond lesion formation, reduced viral replication in the throat may have critical implications in transmission and spread, as Orthopoxviruses traditionally spread through mucosal tissue exposure. Importantly, the 2022 global outbreak resulted from unexpected spread through sexual contact, often at mucosal barriers enriched among men who have sex with men (MSM).⁴⁰ mRNA vaccination resulted in near-complete reduction in systemic viral replication and low-level replication in the throat, with only a transient viral blip between days 11 and 13. This highly significant attenuation of viral replication could potentially lead not only to disease-modifying activity but also to reduced spread. Importantly, enhanced viral control appeared to emerge in the presence of a coordinated role between neutralizing antibodies and antibody effector functions, mediated by FcγR3a and complement to EV antigens. Despite the fact that EVs represent only a small fraction of total produced virions,⁴¹ EV formation is highly conserved across poxviruses, advantageous for viral infection, and represents a key evasive viral progeny. Thus, the data here suggest that additional Fc-mediated functions are likely critical against this specific step of the viral life cycle for full control and clearance of the virus and perhaps essential for limiting spread.

Additional information was obtained on the breadth of the humoral responses after immunization with either mRNA or MVA. IgG binding and functional profiling suggested that immunization with MPXV antigens resulted in the generation of cross-reactive VACV-A27, -A33, -B5, and -L1 and VARV-A31, -A36, -B7, and -M1 antigens, highlighting the broad cross-reactivity that is afforded by immunization with highly conserved MPXV antigens. Moreover, the correlate analyses selected VACV-specific responses, highlighting the highly predictive nature of these cross-reactive responses in predicting viral load and lesion con-

trol. These data imply that an MPXV mRNA vaccine may stimulate antibodies that interact with many Orthopoxvirus species. Conversely, MVA-vaccinated animals showed poor binding titers to the antigens tested, though some responses were observed to three of the four VARV proteins (A33, B5, and L1). Similarly, MVA-immunized animals showed some neutralizing responses to the VACV strains tested but minimal response to the MPXV or other Orthopoxvirus strains tested. However, it is important to note that the focus of humoral responses and Fc-functional activity has been measured against the antigens included in the mRNA vaccine, which were previously reported to be immunodominant after VACV exposure.⁴² Additionally, MVA immunization (within the clinically approved dose range) does provide protection against lethal challenge here and in past animal experiments.¹⁸ We speculate that higher doses of MVA may confer increased immunogenicity and protection. However, manufacturing constraints have rendered it difficult to substantially increase MVA dosing in humans. Given that B cells are necessary for protection, these data argue that MVA-induced humoral immune responses to other antigens may confer protection against death or that MVA-induced humoral VACV-specific immunity is able to evolve rapidly in response to MPXV challenge virus. By contrast, mRNA immunization induces humoral immunity targeting the EV and MV viral surface at the time of challenge that may provide a more robust barrier of immunity, particularly against the pathogenesis of the infection, which can effectively limit viral replication and spread.

The emergence of MPXV as a pathogen able to cause worldwide outbreaks via an increase in sexual transmission, recently reported for the first time for clade I viruses,^{43,44} represents a substantial cause for concern. Strategic drug stockpiles and contemporary vaccines (JYNNEOS) were sufficient to curtail the spread after half a year of circulation with a majority of loss of life avoided, in part due to the low virulence of the clade II strain. However, critically, the 2023–2024 outbreak in Central Africa is currently driven by the more lethal clade I strain of MPXV, with recent reports suggesting that the virus also has the ability to transmit sexually. Lack of vaccine deployment and access to medical countermeasures has fueled the spread of the virus from traditionally endemic rural areas to large metropolitan centers and has led to approximately more than 500 deaths with a case fatality rate of 2.9%. Lack of routine immunization in this region with contemporary VACV-based vaccines appears to have provided fertile ground for continuous low-level spread of the virus and provided an opportunity for mutation, leading to perpetual MPXV outbreaks. Thus, additional safe and highly efficacious vaccine platforms that are rapidly adaptable upon viral mutation are urgently needed to mitigate future outbreaks of MPXV and other zoonotic Orthopoxviruses.

Nucleic-acid vaccines, such as mRNA-LNP vaccine technologies, allow for a rapid response to emerging viral threats. After identifying the etiological agent, sequences against key genes can quickly be synthesized and converted into a potential vaccine with production at regions of interest allowed by worldwide manufacturing centers, particularly in low- and middle-income countries. Moreover, the COVID-19 pandemic illustrated the robust immunogenicity conferred by this platform, resulting in the induction of potent neutralizing antibody titers, durable T cell responses, and durable memory B cell responses.⁴⁵

Fortunately, in the case of poxviruses, researchers have previously down-selected a handful of highly conserved protective targets from the over 200 possible poxviral genes that, when delivered in combination, can be highly efficacious across viruses.^{14,15,20,21,29,46} These studies and additional preclinical data have led to assessment of mRNA-1769 in an ongoing phase I/II clinical trial (NCT05995275) to address the safety and immunogenicity of an mRNA-based Orthopoxvirus vaccine. However, whether additional antigens may be added to drive complete protection and drive protection against additional Orthopoxviruses, whether additional immune responses (for example, T cells) may bolster protection, or whether the induction of immunity, particularly at mucosal barriers, may provide enhanced protection against mucosal challenge remains unclear, but these are all potential avenues for future MPXV mRNA vaccine innovation and testing.

Additionally, longevity of immune responses post-mRNA-1769 immunization has not been measured here. Vaccine kinetics, following all vaccine platforms, typically follow two phases of decay. This includes a phase of rapid antibody decay after peak plasmablast induction, followed by a longer-lived plasma cell response that largely confers durable protection against disease.^{47,48} Along these lines, emerging data from real-world sero-epidemiologic studies suggest that mRNA vaccines induce high peak immune responses that decay but are followed by a second wave of longer-lived plasma-cell-derived antibody responses that are durable against the original encoded SARS-CoV-2 antigens, and this phenomenon has been confirmed with additional mRNA vaccines.^{49,50} Furthermore, studies have also shown that memory B cell responses tend to be stable after mRNA immunization, potentially conferring longer-lived rapid anamnestic responses after viral infection.^{45,51} Yet, whether mRNA vaccines will provide life-long immunity, similar to the remarkable immunity afforded by replicating VACV-based vaccines, remains unclear but will be investigated in an ongoing phase 1/2 trial (NCT05995275) and represents another aspirational goal for future pandemic-curbing mRNA vaccines to novel Orthopoxviral pathogens and beyond.

Limitations of the study

This study describes an observational and immunological comparison of mRNA and MVA vaccines in an NHP model of lethal MPXV infection via IV administration. The doses selected in this study were based on relevant human doses, but a range of doses would be ideal to further profile the immune response at a higher resolution. IV administration is thought to best replicate the natural course of disease as it presents during infection in the human population, but exploration of additional routes of administration may offer different lenses to explore immune correlates of transmission and disease. Cellular immune analysis was not included in this study to compare across vaccine types and will be included in future studies both pre-clinically and clinically.

RESOURCE AVAILABILITY

Lead contact

Further information and requests for resources and reagents should be directed to and will be fulfilled by the lead contact, Jay Hooper (jay.w.hooper.civ@health.mil).

Materials availability

There are restrictions to the availability of mRNA-1769, which requires a material transfer agreement with Moderna for use.

Data and code availability

- All original code has been deposited at Zenodo and is publicly available as of the date of publication. DOIs are listed in the [key resources table](#). Original data has been deposited in Mendeley Data and is publicly available as of the date of publication.
- Any additional information required to reanalyze the data reported in this paper is available from the [lead contact](#) upon request.

ACKNOWLEDGMENTS

We would like to thank Dave Dyer and Ondraya Frick for study specimen logistics, USAMRIID Veterinary Medicine Division and Pathology Division personnel for their specialized support, and Sarah Norris for statistical analysis. We would also like to thank the team at Battelle Memorial Institute for their technical assistance with ECTV. Some figures were produced using BioRender. N.J.S. received funding from the Trustees of Boston University, and funding for P.L.E., J.L.A., C.A.C., and B.M. was provided by the Division of Intramural Research and NIAID.

AUTHOR CONTRIBUTIONS

Conceptualization, A.W.F., A.C., W.-H.Y., N.J.S., B.M., G.A., and J.W.H.; methodology, E.M.M., S.L.B., C.A., P.L.E., H.N., G.S., T.R.F., G.A.A., D.S., P.A.J., K.H., and W.-H.Y.; formal analysis, D.C.; investigation, E.M.M., S.L.B., C.A., P.L.E., H.N., G.S., T.R.F., R.H.L., A.M., G.A.A., J.L.A., C.A.C., J.W.K., C.I.D., J.D.S., K.O., J.L.R., and K.M.R.; resources, E.M.M., A.W.F., D.C., C.A., P.L.E., R.H.L., A.M., G.A.A., and K.H.; writing – original draft, E.M.M., A.W.F., G.A., and J.W.H.; writing – review and editing, E.M.M., A.W.F., S.L.B., D.C., W.-H.Y., N.J.S., B.M., G.A., and J.W.H.; visualization, E.M.M., A.W.F., D.C., C.A., and H.N.; supervision, A.W.F., A.C., W.-H.Y., N.J.S., B.M., G.A., and J.W.H.; project administration, J.C.J.; funding acquisition, A.C., B.M., and J.W.H.

DECLARATION OF INTERESTS

Opinions, interpretations, conclusions, and recommendations are those of the authors and are not necessarily endorsed by the US Army. A.W.F., D.C., C.A., H.N., G.S., T.R.F., R.H.L., A.M., G.A.A., D.S., P.A.J., H.B., J.C.J., K.H., A.C., W.-H.Y., and G.A. are employees of Moderna. G.A. is an equity holder in Systems Seromyx and Leyden Labs and has received collaborative funding from Moderna, GSK, Sanofi, Medicago, BioNtech, Clover, and Pfizer in the past year. P.L.E., J.L.A., C.A.C., and B.M. were supported by the Division of Intramural Research, NIAID, NIH.

STAR★METHODS

Detailed methods are provided in the online version of this paper and include the following:

- [KEY RESOURCES TABLE](#)
- [EXPERIMENTAL MODEL AND STUDY PARTICIPANT DETAILS](#)
 - Nonhuman primates
 - Cells
 - Viruses
- [METHOD DETAILS](#)
 - Vaccine compositions
 - Vaccination of nonhuman primates
 - Lesional MPXV model in nonhuman primates
 - Infectious viral titrations
 - Quantitation of MPXV nucleic acid
 - Luminex assay
 - MAGPIX and recombinant antigens
 - Lysed MVA ELISA

- PRNT for the MV form of poxviruses
- PRNT for the EV form of poxviruses
- GFP-expressing VACV and MPXV neutralization
- Antibody-dependent complement deposition
- Antibody-dependent cellular phagocytosis
- Antibody-dependent neutrophil phagocytosis
- Antibody-dependent NK cell activation
- **QUANTIFICATION AND STATISTICAL ANALYSIS**
 - Unsupervised clustering of vaccine signature
 - Correlates analyses
 - Correlation network analysis

Received: December 19, 2023

Revised: August 9, 2024

Accepted: August 21, 2024

Published: September 4, 2024

REFERENCES

1. Koplan, J.P., and Foster, S.O. (1979). Smallpox: clinical types, causes of death, and treatment. *J. Infect. Dis.* *140*, 440–441. <https://doi.org/10.1093/infdis/140.3.440>.
2. Breman, J.G., Kalisa-Ruti, R., Steniowski, M.V., Zanotto, E., Gromyko, A.I., and Arita, I. (1980). Human monkeypox, 1970–79. *Bull. World Health Organ.* *58*, 165–182.
3. About Mpox (2024). <https://www.cdc.gov/poxvirus/mpox/about/index.html#:~:text=The%20Clade%20I%20type%20of,disease%20are%20likely%20to%20survive>.
4. Rimoin, A.W., Mulembakani, P.M., Johnston, S.C., Lloyd Smith, J.O.L., Kishalu, N.K., Kinkela, T.L., Blumberg, S., Thomassen, H.A., Pike, B.L., Fair, J.N., et al. (2010). Major increase in human monkeypox incidence 30 years after smallpox vaccination campaigns cease in the Democratic Republic of Congo. *Proc. Natl. Acad. Sci. USA* *107*, 16262–16267. <https://doi.org/10.1073/pnas.1005769107>.
5. 2022–2024 Mpox (Monkeypox) Outbreak: Global Trends. https://worldhealthorg.shinyapps.io/mpox_global.
6. Deputy, N.P., Deckert, J., Chard, A.N., Sandberg, N., Moulia, D.L., Barkley, E., Dalton, A.F., Sweet, C., Cohn, A.C., Little, D.R., et al. (2023). Vaccine Effectiveness of JYNNEOS against Mpox Disease in the United States. *N. Engl. J. Med.* *388*, 2434–2443. <https://doi.org/10.1056/NEJMoa2215201>.
7. Rosenberg, E.S., Dorabawila, V., Hart-Malloy, R., Anderson, B.J., Miranda, W., O'Donnell, T., Gonzalez, C.J., Abrego, M., DelBarba, C., Tice, C.J., et al. (2023). Effectiveness of JYNNEOS Vaccine Against Diagnosed Mpox Infection - New York, 2022. *MMWR Morb. Mortal. Wkly. Rep.* *72*, 559–563. <https://doi.org/10.15585/mmwr.mm7220a4>.
8. Dalton, A.F., Diallo, A.O., Chard, A.N., Moulia, D.L., Deputy, N.P., Fothergill, A., Kracalik, I., Wegner, C.W., Markus, T.M., Pathela, P., et al. (2023). Estimated Effectiveness of JYNNEOS Vaccine in Preventing Mpox: A Multijurisdictional Case-Control Study - United States. *MMWR Morb. Mortal. Wkly. Rep.* *72*, 553–558. <https://doi.org/10.15585/mmwr.mm7220a3>.
9. Lin, Y.-C., Wen, T.-H., Shih, W.-L., Vermund, S.H., and Fang, C.-T. (2024). Impact of vaccination and high-risk group awareness on the mpox epidemic in the United States, 2022–2023: a modelling study. *EClinical medicine* *68*, 102407. <https://doi.org/10.1016/j.eclinm.2023.102407>.
10. European Centre for Disease Prevention and Control (2024). Outbreak of mpox caused by Monkeypox virus clade I in the Democratic Republic of the Congo. <https://www.ecdc.europa.eu/en/news-events/outbreak-mpox-caused-monkeypox-virus-clade-i-democratic-republic-congo>.
11. Wolff Sagy, Y., Zucker, R., Hammerman, A., Markovits, H., Arieh, N.G., Abu Ahmad, W., Battat, E., Ramot, N., Carmeli, G., Mark-Amir, A., et al. (2023). Real-world effectiveness of a single dose of mpox vaccine in males. *Nat. Med.* *29*, 748–752. <https://doi.org/10.1038/s41591-023-02229-3>.
12. Hogan, M.J., and Pardi, N. (2022). mRNA Vaccines in the COVID-19 Pandemic and Beyond. *Annu. Rev. Med.* *73*, 17–39. <https://doi.org/10.1146/annurev-med-042420-112725>.
13. Pardi, N., Hogan, M.J., Porter, F.W., and Weissman, D. (2018). mRNA vaccines - a new era in vaccinology. *Nat. Rev. Drug Discov.* *17*, 261–279. <https://doi.org/10.1038/nrd.2017.243>.
14. Hooper, J.W., Custer, D.M., and Thompson, E. (2003). Four-gene-combination DNA vaccine protects mice against a lethal vaccinia virus challenge and elicits appropriate antibody responses in nonhuman primates. *Virology* *306*, 181–195. [https://doi.org/10.1016/s0042-6822\(02\)00038-7](https://doi.org/10.1016/s0042-6822(02)00038-7).
15. Hooper, J.W., Thompson, E., Wilhelmson, C., Zimmerman, M., Ichou, M.A., Steffen, S.E., Schmaljohn, C.S., Schmaljohn, A.L., and Jahrling, P.B. (2004). Smallpox DNA vaccine protects nonhuman primates against lethal monkeypox. *J. Virol.* *78*, 4433–4443. <https://doi.org/10.1128/jvi.78.9.4433-4443.2004>.
16. Lustig, S., Fogg, C., Whitbeck, J.C., Eisenberg, R.J., Cohen, G.H., and Moss, B. (2005). Combinations of polyclonal or monoclonal antibodies to proteins of the outer membranes of the two infectious forms of vaccinia virus protect mice against a lethal respiratory challenge. *J. Virol.* *79*, 13454–13462. <https://doi.org/10.1128/JVI.79.21.13454-13462.2005>.
17. Golden, J.W., Zaitseva, M., Kapnick, S., Fisher, R.W., Mikolajczyk, M.G., Ballantyne, J., Golding, H., and Hooper, J.W. (2011). Polyclonal antibody cocktails generated using DNA vaccine technology protect in murine models of orthopoxvirus disease. *Virol. J.* *8*, 441. <https://doi.org/10.1186/1743-422X-8-441>.
18. Edghill-Smith, Y., Golding, H., Manischewitz, J., King, L.R., Scott, D., Bray, M., Nalca, A., Hooper, J.W., Whitehouse, C.A., Schmitz, J.E., et al. (2005). Smallpox vaccine-induced antibodies are necessary and sufficient for protection against monkeypox virus. *Nat. Med.* *11*, 740–747. <https://doi.org/10.1038/nm1261>.
19. Heraud, J.M., Edghill-Smith, Y., Ayala, V., Kalisz, I., Parrino, J., Kalyanaraman, V.S., Manischewitz, J., King, L.R., Hryniewicz, A., Trindade, C.J., et al. (2006). Subunit recombinant vaccine protects against monkeypox. *J. Immunol.* *177*, 2552–2564. <https://doi.org/10.4049/jimmunol.177.4.2552>.
20. Freyn, A.W., Atyeo, C., Earl, P.L., Americo, J.L., Chuang, G.Y., Natarajan, H., Frey, T.R., Gall, J.G., Moliva, J.I., Hunegnaw, R., et al. (2023). An mpox virus mRNA-lipid nanoparticle vaccine confers protection against lethal orthopoxviral challenge. *Sci. Transl. Med.* *15*, eadg3540. <https://doi.org/10.1126/scitranslmed.adg3540>.
21. Sang, Y., Zhang, Z., Liu, F., Lu, H., Yu, C., Sun, H., Long, J., Cao, Y., Mai, J., Miao, Y., et al. (2023). Monkeypox virus quadrivalent mRNA vaccine induces immune response and protects against vaccinia virus. *Signal Transduct. Target. Ther.* *8*, 172. <https://doi.org/10.1038/s41392-023-01432-5>.
22. Payne, A.B., Ray, L.C., Cole, M.M., Canning, M., Houck, K., Shah, H.J., Farrar, J.L., Lewis, N.M., Fothergill, A., White, E.B., et al. (2022). Reduced Risk for Mpox After Receipt of 1 or 2 Doses of JYNNEOS Vaccine Compared with Risk Among Unvaccinated Persons - 43 U.S. Jurisdictions, July 31–October 1, 2022. *MMWR Morb. Mortal. Wkly. Rep.* *71*, 1560–1564. <https://doi.org/10.15585/mmwr.mm7149a5>.
23. Antoine, G., Scheiffinger, F., Dorner, F., and Falkner, F.G. (1998). The complete genomic sequence of the modified vaccinia Ankara strain: comparison with other orthopoxviruses. *Virology* *244*, 365–396. <https://doi.org/10.1006/viro.1998.9123>.
24. Xiao, Y., Zeng, Y., Schante, C., Joshi, S.B., Buchman, G.W., Volkin, D.B., Middaugh, C.R., and Isaacs, S.N. (2020). Short-term and longer-term protective immune responses generated by subunit vaccination with smallpox A33, B5, L1 or A27 proteins adjuvanted with aluminum hydroxide and CpG in mice challenged with vaccinia virus. *Vaccine* *38*, 6007–6018. <https://doi.org/10.1016/j.vaccine.2020.07.018>.
25. Cann, J.A., Jahrling, P.B., Hensley, L.E., and Wahl-Jensen, V. (2013). Comparative Pathology of Smallpox and Monkeypox in Man and Macaques. *J. Comp. Pathol.* *148*, 6–21. <https://doi.org/10.1016/j.jcpa.2012.06.007>.

26. Parker, S., and Buller, R.M. (2013). A review of experimental and natural infections of animals with monkeypox virus between 1958 and 2012. *Future Virol.* 8, 129–157. <https://doi.org/10.2217/fvl.12.130>.
27. Benhnia, M.R.E.I., McCausland, M.M., Moyron, J., Laudenslager, J., Granger, S., Rickert, S., Koriazova, L., Kubo, R., Kato, S., and Crotty, S. (2009). Vaccinia virus extracellular enveloped virion neutralization in vitro and protection in vivo depend on complement. *J. Virol.* 83, 1201–1215. <https://doi.org/10.1128/JVI.01797-08>.
28. Africa CDC (2024). *Weekly Event Based Surveillance Report*.
29. Zuiani, A., Dulberger, C.L., De Silva, N.S.D., Marquette, M., Lu, Y.-J., Palowitch, G.M., Dokic, A., Sanchez-Velazquez, R., Schlatterer, K., Sarkar, S., et al. (2024). A multivalent mRNA monkeypox virus vaccine (BNT166) protects mice and macaques from orthopoxvirus disease. *Cell* 187, 1363–1373.e12. <https://doi.org/10.1016/j.cell.2024.01.017>.
30. Hubert, M., Guivel-Benhassine, F., Bruel, T., Porrot, F., Planas, D., Vanhomwegen, J., Wiedemann, A., Burrel, S., Marot, S., Palich, R., et al. (2023). Complement-dependent mpox-virus-neutralizing antibodies in infected and vaccinated individuals. *Cell Host Microbe* 31, 937–948.e4. <https://doi.org/10.1016/j.chom.2023.05.001>.
31. Earl, P.L., Americo, J.L., and Moss, B. (2020). Natural killer cells expanded in vivo or ex vivo with IL-15 overcomes the inherent susceptibility of CAST mice to lethal infection with orthopoxviruses. *PLoS Pathog.* 16, e1008505. <https://doi.org/10.1371/journal.ppat.1008505>.
32. Sukhdeo, S., Mishra, S., and Walmsley, S. (2022). Human monkeypox: a comparison of the characteristics of the new epidemic to the endemic disease. *BMC Infect. Dis.* 22, 928. <https://doi.org/10.1186/s12879-022-07900-7>.
33. Parrino, J., McCurdy, L.H., Larkin, B.D., Gordon, I.J., Rucker, S.E., Enama, M.E., Koup, R.A., Roederer, M., Bailer, R.T., Moodie, Z., et al. (2007). Safety, immunogenicity and efficacy of modified vaccinia Ankara (MVA) against Dryvax challenge in vaccinia-naïve and vaccinia-immune individuals. *Vaccine* 25, 1513–1525. <https://doi.org/10.1016/j.vaccine.2006.10.047>.
34. Wyatt, L.S., Earl, P.L., Eller, L.A., and Moss, B. (2004). Highly attenuated smallpox vaccine protects mice with and without immune deficiencies against pathogenic vaccinia virus challenge. *Proc. Natl. Acad. Sci. USA* 101, 4590–4595. <https://doi.org/10.1073/pnas.0401165101>.
35. Berens-Riha, N., Block, T.D., Rutgers, J., Michiels, J., Gestel, L.V., Hens, M., I.T.M. monkeypox study, Kenyon, C., Bottieau, E., Soentjens, P., et al. (2022). Severe mpox (formerly monkeypox) disease in five patients after recent vaccination with MVA-BN vaccine, Belgium, July to October 2022. *Eurosurveillance* 27, 2200894. <https://doi.org/10.2807/1560-7917.es.2022.27.48.2200894>.
36. Taha, A.M., Rodriguez-Morales, A.J., and Sah, R. (2023). Mpox breakthrough infections: concerns and actions. *Lancet Infect. Dis.* 23, 1216–1218. [https://doi.org/10.1016/S1473-3099\(23\)00546-7](https://doi.org/10.1016/S1473-3099(23)00546-7).
37. Polack, F.P., Thomas, S.J., Kitchin, N., Absalon, J., Gurtman, A., Lockhart, S., Perez, J.L., Pérez Marc, G.P., Moreira, E.D., Zerbini, C., et al. (2020). Safety and Efficacy of the BNT162b2 mRNA Covid-19 Vaccine. *N. Engl. J. Med.* 383, 2603–2615. <https://doi.org/10.1056/NEJMoa2034577>.
38. Jackson, L.A., Anderson, E.J., Roupael, N.G., Roberts, P.C., Makhene, M., Coler, R.N., McCullough, M.P., Chappell, J.D., Denison, M.R., Stevens, L.J., et al. (2020). An mRNA Vaccine against SARS-CoV-2 - Preliminary Report. *N. Engl. J. Med.* 383, 1920–1931. <https://doi.org/10.1056/NEJMoa2022483>.
39. Peng, F., Hu, N., Liu, Y., Xing, C., Luo, L., Li, X., Wang, J., Chen, G., Xiao, H., Liu, C., et al. (2023). Functional epitopes and neutralizing antibodies of vaccinia virus. *Front. Microbiol.* 14, 1255935. <https://doi.org/10.3389/fmicb.2023.1255935>.
40. Tarín-Vicente, E.J., Alemany, A., Agud-Dios, M., Ubals, M., Suñer, C., Antón, A., Arando, M., Arroyo-Andrés, J., Calderón-Lozano, L., Casañ, C., et al. (2022). Clinical presentation and virological assessment of confirmed human monkeypox virus cases in Spain: a prospective observational cohort study. *Lancet* 400, 661–669. [https://doi.org/10.1016/S0140-6736\(22\)01436-2](https://doi.org/10.1016/S0140-6736(22)01436-2).
41. Pickup, D.J. (2015). Extracellular Virions: The Advance Guard of Poxvirus Infections. *PLoS Pathog.* 11, e1004904. <https://doi.org/10.1371/journal.ppat.1004904>.
42. Gilchuk, I., Gilchuk, P., Sapparapu, G., Lampley, R., Singh, V., Kose, N., Blum, D.L., Hughes, L.J., Satheshkumar, P.S., Townsend, M.B., et al. (2016). Cross-Neutralizing and Protective Human Antibody Specificities to Poxvirus Infections. *Cell* 167, 684–694.e9. <https://doi.org/10.1016/j.cell.2016.09.049>.
43. Kibungu, E.M., Vakaniaki, E.H., Kinganda-Lusamaki, E., Kalonji-Mukendi, T., Pukuta, E., Hoff, N.A., Bogoch, I.I., Cevik, M., Gonsalves, G.S., Hensley, L.E., et al. (2024). Clade I-Associated Mpox Cases Associated with Sexual Contact, the Democratic Republic of the Congo. *Emerging Infect. Dis.* 30, 172–176. <https://doi.org/10.3201/eid3001.231164>.
44. Masirika, L.M., Udahemuka, J.C., Schuele, L., Ndishimye, P., Otani, S., Mbiribindi, J.B., Marekani, J.M., Mambo, L.M., Bubala, N.M., Boter, M., et al. (2024). Ongoing mpox outbreak in Kamituga, South Kivu province, associated with monkeypox virus of a novel Clade I sub-lineage, Democratic Republic of the Congo, 2024. *Euro Surveill.* 29, 2400106. <https://doi.org/10.2807/1560-7917.ES.2024.29.11.2400106>.
45. Goel, R.R., Painter, M.M., Apostolidis, S.A., Mathew, D., Meng, W., Rosenfeld, A.M., Lundgreen, K.A., Reynaldi, A., Khoury, D.S., Pattekar, A., et al. (2021). mRNA vaccines induce durable immune memory to SARS-CoV-2 and variants of concern. *Science* 374, abm0829. <https://doi.org/10.1126/science.abm0829>.
46. Mucker, E.M., Golden, J.W., Hammerbeck, C.D., Kishimori, J.M., Royals, M., Joselyn, M.D., Ballantyne, J., Nalca, A., and Hooper, J.W. (2022). A Nucleic Acid-Based Orthopoxvirus Vaccine Targeting the Vaccinia Virus L1, A27, B5, and A33 Proteins Protects Rabbits against Lethal Rabbitpox Virus Aerosol Challenge. *J. Virol.* 96, e01504-21. <https://doi.org/10.1128/JVI.01504-21>.
47. Alter, G., and Seder, R. (2020). The Power of Antibody-Based Surveillance. *N. Engl. J. Med.* 383, 1782–1784. <https://doi.org/10.1056/NEJMe2028079>.
48. Amanna, I.J., Carlson, N.E., and Slifka, M.K. (2007). Duration of Humoral Immunity to Common Viral and Vaccine Antigens. *N. Engl. J. Med.* 357, 1903–1915. <https://doi.org/10.1056/NEJMoa066092>.
49. Essink, B., Chu, L., Seger, W., Barranco, E., Le Cam, N.L., Bennett, H., Faughnan, V., Pajon, R., Paila, Y.D., Bollman, B., et al. (2023). The safety and immunogenicity of two Zika virus mRNA vaccine candidates in healthy flavivirus baseline seropositive and seronegative adults: the results of two randomised, placebo-controlled, dose-ranging, phase 1 clinical trials. *Lancet Infect. Dis.* 23, 621–633. [https://doi.org/10.1016/S1473-3099\(22\)00764-2](https://doi.org/10.1016/S1473-3099(22)00764-2).
50. Srivastava, K., Carreño, J.M., Gleason, C., Monahan, B., Singh, G., Abbad, A., Tcheou, J., Raskin, A., Kleiner, G., Bakel, H. van, et al. (2024). SARS-CoV-2-infection- and vaccine-induced antibody responses are long lasting with an initial waning phase followed by a stabilization phase. *Immunity* 57, 587–599.e4. <https://doi.org/10.1016/j.immuni.2024.01.017>.
51. Gagne, M., Corbett, K.S., Flynn, B.J., Foulds, K.E., Wagner, D.A., Andrew, S.F., Todd, J.-P.M., Honeycutt, C.C., McCormick, L., Nurmukhambetova, S.T., et al. (2022). Protection from SARS-CoV-2 Delta one year after mRNA-1273 vaccination in rhesus macaques coincides with anamnestic antibody response in the lung. *Cell* 185, 113–130.e15. <https://doi.org/10.1016/j.cell.2021.12.002>.
52. Mucker, E.M., Lindquist, M., and Hooper, J.W. (2020). Particle-specific neutralizing activity of a monoclonal antibody targeting the poxvirus A33 protein reveals differences between cell associated and extracellular enveloped virions. *Virology* 544, 42–54. <https://doi.org/10.1016/j.virol.2020.02.004>.
53. Mucker, E.M., Shamblin, J.D., Raymond, J.L., Twenhafel, N.A., Garry, R.F., and Hensley, L.E. (2022). Effect of Monkeypox Virus Preparation on the Lethality of the Intravenous Cynomolgus Macaque Model. *Viruses* 14, 1741. <https://doi.org/10.3390/v14081741>.

54. Likos, A.M., Sammons, S.A., Olson, V.A., Frace, A.M., Li, Y., Olsen-Rasmussen, M., Davidson, W., Galloway, R., Khristova, M.L., Reynolds, M.G., et al. (2005). A tale of two clades: monkeypox viruses. *J. Gen. Virol.* 86, 2661–2672. <https://doi.org/10.1099/vir.0.81215-0>.
55. Earl, P.L., Americo, J.L., and Moss, B. (2003). Development and Use of a Vaccinia Virus Neutralization Assay Based on Flow Cytometric Detection of Green Fluorescent Protein. *J. Virol.* 77, 10684–10688. <https://doi.org/10.1128/jvi.77.19.10684-10688.2003>.
56. Mudhasani, R.R., Golden, J.W., Adam, G.C., Hartingh, T.J., Kota, K.P., Ordonez, D., Quackenbush, C.R., Tran, J.P., Cline, C., Williams, J.A., et al. (2024). Orally available nucleoside analog UMM-766 provides protection in a murine model of orthopox disease. *Microbiol. Spectr.* 12, e03586-23. <https://doi.org/10.1128/spectrum.03586-23>.
57. Smee, D.F., Sidwell, R.W., Kefauver, D., Bray, M., and Huggins, J.W. (2002). Characterization of Wild-Type and Cidofovir-Resistant Strains of Camelpox, Cowpox, Monkeypox, and Vaccinia Viruses. *Antimicrob. Agents Chemother.* 46, 1329–1335. <https://doi.org/10.1128/AAC.46.5.1329-1335.2002>.
58. Smee, D.F., Bailey, K.W., and Sidwell, R.W. (2002). Treatment of lethal cowpox virus respiratory infections in mice with 2-amino-7-[[1,3-dihydroxy-2-propoxy)methyl]purine and its orally active diacetate ester prodrug. *Antiviral Res.* 54, 113–120. [https://doi.org/10.1016/s0166-3542\(01\)00217-0](https://doi.org/10.1016/s0166-3542(01)00217-0).
59. Mucker, E.M., Shamblin, J.D., Goff, A.J., Bell, T.M., Reed, C., Twenhafel, N.A., Chapman, J., Mattix, M., Alves, D., Garry, R.F., and Hensley, L.E. (2022). Evaluation of Virulence in Cynomolgus Macaques Using a Virus Preparation Enriched for the Extracellular Form of Monkeypox Virus. *Viruses* 14, 1993. <https://doi.org/10.3390/v14091993>.
60. Moss, B. (2021). *DNA Viruses* (Wolters Kluwer).
61. Hooper, J.W., Custer, D.M., Schmaljohn, C.S., and Schmaljohn, A.L. (2000). DNA Vaccination with Vaccinia Virus L1R and A33R Genes Protects Mice against a Lethal Poxvirus Challenge. *Virology* 266, 329–339. <https://doi.org/10.1006/viro.1999.0096>.
62. Fischinger, S., Fallon, J.K., Michell, A.R., Broge, T., Suscovich, T.J., Streeck, H., and Alter, G. (2019). A high-throughput, bead-based, antigen-specific assay to assess the ability of antibodies to induce complement activation. *J. Immunol. Methods* 473, 112630. <https://doi.org/10.1016/j.jim.2019.07.002>.
63. Karsten, C.B., Mehta, N., Shin, S.A., Diefenbach, T.J., Slein, M.D., Karpinski, W., Irvine, E.B., Broge, T., Suscovich, T.J., and Alter, G. (2019). A versatile high-throughput assay to characterize antibody-mediated neutrophil phagocytosis. *J. Immunol. Methods* 471, 46–56. <https://doi.org/10.1016/j.jim.2019.05.006>.
64. Atyeo, C.G., Shook, L.L., Brigida, S., De Guzman, R.M.D., Demidkin, S., Muir, C., Akinwunmi, B., Baez, A.M., Sheehan, M.L., McSweeney, E., et al. (2022). Maternal immune response and placental antibody transfer after COVID-19 vaccination across trimester and platforms. *Nat. Commun.* 13, 3571. <https://doi.org/10.1038/s41467-022-31169-8>.

STAR★METHODS

KEY RESOURCES TABLE

REAGENT or RESOURCE	SOURCE	IDENTIFIER
Antibodies		
anti-guinea pig complement C3	MP Biomedicals	Cat# MP0855385; RRID: AB_2334913
monoclonal antibody, anti-poxvirus L1	USAMRIID	7D11
anti-CD66b PacBlue	Biolegend	Cat# 305112; RRID: AB_2563294
Monoclonal antibody, anti-poxvirus A33	Mucker et al. ⁵²	C6C
Monoclonal antibody, anti-poxvirus B5	Mucker et al. ⁵²	C8a
anti-CD107a BV605 (clone H4A3)	Biolegend	Cat# 328634; RRID: AB_2563851
anti-CD56 APC (clone MEM-188)	Biolegend	Cat# 304610; RRID: AB_314452
anti-CD3 APC-Cy7 (clone UCHT1)	Biolegend	Cat# 300426; RRID: AB_830755
anti-MIP1b-BV421 (clone D21-1351)	BD Biosciences	Cat# 562900; RRID: AB_2737877
anti-IFN γ -PE (clone B27)	Biolegend	Cat# 506507; RRID: AB_315440
goat anti-human	Sigma Aldrich	Cat# 401954; RRID: AB_212016
anti-rhesus IgG-PE	Southern Biotech	Cat# 6200-09; RRID: AB_2796270
anti-rhesus IgA-biotin (clone 10F12)	NHP Reagent Resource	Cat# PR-0126; RRID: AB_2819304
anti-rhesus IgG1-biotin (clone 7H11)	NHP Reagent Resource	Cat# PR-7116; RRID: AB_2819311
anti-rhesus IgG2-biotin (clone dio)	NHP Reagent Resource	Cat# PR-0003; RRID: AB_2895608
anti-rhesus IgG3-biotin (clone tria)	NHP Reagent Resource	Cat# PR-0006; RRID: AB_2895616
anti-rhesus IgG4-biotin (clone 7A8)	NHP Reagent Resource	Cat# PR-7186; RRID: AB_2819323
Bacterial and virus strains		
Clade I MPXV Zaire '79 (V79-I-005)	Mucker et al. ⁵³	N/A
Clade IIA MPXV, US 2003	Likos et al. ⁵⁴	USAMRIID
Recombinant Vaccinia virus strain WR-GFP	Earl et al. ⁵⁵	NIAID
Recombinant MPXV-GFP	Frey et al. ²⁰	NIAID
Vaccinia virus, strain WR (BEI NR-55)	Mudhasani et al. ⁵⁶	Biodefense Reference Material Repository
MVA Modified Vaccinia Ankara	Wyatt et al. ³⁴	N/A
Rabbitpox virus, Utrecht (ATCC VR1591)	Mudhasani et al. ⁵⁶	Biodefense Reference Material Repository
Camelpox virus, strain Somalia	Smee et al. ⁵⁷	USAMRIID
Ectromelia virus, Moscow	BEI Resources	Cat# VR-1374
Biological samples		
Human complement	Cedarlane	Cat# CL6600
Guinea pig complement	Cedarlane	Cat# CL5000
Chemicals, peptides, and recombinant proteins		
Orthopoxvirus mRNA-LNP vaccine	Frey et al. ²⁰	mRNA-1769
Magpix vaccinia virus and MPXV antigens	Hooper et al. ^{14,15} and Heraud et al. ¹⁹	A27/A29, A33/A35, B5/B6 and L1
VACV, MPXV, and VARV recombinant proteins	Frey et al. ²⁰	A27/A29/A31, A33/A35/A36, B5/B6/B7, and L1/M1/M1
Rhesus Fc gamma Receptor IIa-biotin	Sino Biological	Cat# 90016-K49H-B
Rhesus Fc gamma Receptor IIIa-biotin	Sino Biological	Cat# 90013-C27H-B
Critical commercial assays		
xMAP coupling kits	Luminex	Cat# 4050016
TaqPath 1 Step RTqPCR Master Mix	ThermoFisher Scientific	Cat# A15299
FluoSpheres NeutrAvidin-Labeled Microspheres	Invitrogen	Cat# F8776

(Continued on next page)

Continued		
REAGENT or RESOURCE	SOURCE	IDENTIFIER
Deposited data		
Data availability	Mendeley Data	https://doi.org/10.17632/7pwgvpwf9b.2
Code availability	Zenodo	https://doi.org/10.5281/zenodo.12865619
Experimental models: Cell lines		
Vero E6	ATCC	Cat# CRL-1586; RRID: CVCL_0574
HEK293T	ATCC	Cat# CRL-3216; RRID: CVCL_0063
Vero 76	ATCC	Cat# CRL-1587; RRID: CVCL_0603
Hela S3	ATCC	Cat# CCL2.2; RRID: CVCL_0058
Experimental models: Organisms/strains		
Cynomolgus macaques (<i>Macaca fascicularis</i>)	WorldWide Primates Inc	N/A
Oligonucleotides		
MPXV qRT-PCR Forward primer	5'-CTCATTGATTTTTCGCGGGATA	MPOX-F3L-F290
MPXV qRT-PCR Reverse Primer	5'-ACGATACTCCTCCTMGTTGGTC	MPOX-F3L-R396a
MPXV qRT-PCR probe	FAM-CATCAGAATCTGTAGGCCGT-MGBNFQ)	MPOX-F3L-p333
Software and algorithms		
Graphpad Prism	GraphPad Software, LLC	Version 9.4
Flow Jo	BD Sciences	N/A
Flexmap 3D	Luminex	N/A

EXPERIMENTAL MODEL AND STUDY PARTICIPANT DETAILS

Nonhuman primates

Eighteen male cynomolgus macaques of Cambodian origins were randomized by a statistician into three vaccination groups of 6 animals each, stratified by weight. All animals weighed between 3.7 and 6.3 kilograms at study start, except one animal which weighed 9.1 kilograms and was placed in the control group. All NHPs were 6 to 8 years of age and were research naïve and determined to be healthy by veterinarian examination prior to study start. Research was conducted in a BSL-3 facility with animals single housed and all work was performed under an IACUC approved protocol at USAMRIID (USDA Registration Number 51-F-00211728 & OLAW Assurance Number A3473-01) in compliance with the Animal Welfare Act and other federal statutes and regulations relating to animals and experiments involving animals. The facility where this research was conducted is fully accredited by the Association for Assessment and Accreditation of Laboratory Animal Care International and adheres to principles stated in the Guide for the Care and Use of Laboratory Animals, National Research Council, 2011. All manipulations involving MPXV were performed under BSL-3 conditions.

Cells

Cells used in immunoassays included Vero E6 (ATCC CRL-1586, female), HEK 293T (ATCC CRL-3216, female), and Vero 76 (ATCC, CRL-1587, female) and were maintained by USAMRIID Virology Division using standard procedures at 37°C and 5% CO₂. HeLa S3 cells (ATCC CCL2.2, female) were utilized for VACV-GFP and MPXV GFP neutralization assays and maintained using standard procedures at 37°C and 5% CO₂. Cell line authentication was not performed for this study.

Viruses

MPXV Clade I (Zaire '79) was propagated as previously reported.⁵³ West African MPXV US 2003-044 was obtained during the 2003 US outbreak from the lymph node of an infected prairie dog associated with the initial case⁵⁴; the virus was passaged three times in BSC-40 cells and twice in MA-104 cells. The Somalia strain of camelpox virus was obtained by USAMRIID from Joseph Esposito, Centers for Disease Control and Prevention, Atlanta, GA and stocks generated.⁵⁸ Vaccinia virus strain WR and rabbitpox virus were received from BEI Resources and propagated at USAMRIID as previously reported.⁵⁶

ECTV was obtained from BEI Resources and propagated at Battelle Memorial Institute. VACV WR GFP and MPXV Zaire 79 GFP were previously described.^{20,55}

METHOD DETAILS

Vaccine compositions

mRNA encoding equal concentrations of four MPXV Clade IIb genes, A35R, M1R, A29L, and B6R, were provided by Moderna (mRNA-1769) and maintained at $-80^{\circ}\text{C} \pm 10^{\circ}\text{C}$. mRNA-1769 was thawed for vaccine preparation and diluted in ice cold 1X PBS without calcium/magnesium (Corning) to a target of 150 $\mu\text{g}/\text{dose}$ for intramuscular (IM) administration. Dose selection was based on previous acceptable safety data for SM102 formulated mRNA-LNP vaccines. Modified Vaccinia Ankara vaccine was previously described³⁴ and stored at $-80^{\circ}\text{C} \pm 10^{\circ}\text{C}$. MVA was thawed and diluted in ice cold 1X PBS before vaccination. A target dose of 0.7×10^8 PFU/dose was administered via the subcutaneous (SC) route. This dose was based on the human dose of licensed MVA-based vaccines (0.5×10^8 to 3.95×10^8 infectious units per 0.5 mL dose).

Vaccination of nonhuman primates

Investigators performing observations were blinded to the specific group designation of the nonhuman primates. Prior to vaccination, animals were confirmed to be negative for antibodies against orthopoxviruses by assessment of binding titers. Vaccinations, physical examinations, blood collection, and intravenous MPXV challenge were administered under anesthesia (10 mg/kg ketamine or 3 mg/kg tiletamine-zolazepam). Animals were vaccinated with either mRNA-1769, MVA, or an equal volume (0.5mL) of 1X PBS on day 0 and day 26 (Figure 1). Vaccines were administered by intramuscular (mRNA-1769 or mock) or subcutaneous (MVA) injection within or above the deltoid muscle, respectively. Right and left deltoids were used for day 0 and day 26, respectively. Blood samples for immunogenicity assays were collected as annotated in Figure 1.

Lesional MPXV model in nonhuman primates

For efficacy testing, the cynomolgus lesional (intravenous) model of mpox and smallpox was utilized as previously described.⁵⁹ On day 53, animals were transported into animal biosafety level-3 (ABSL-3) for MPXV challenge. Briefly, 56 days after the first vaccination, animals were exposed to a target intravenous dose of 5×10^7 PFU of clade I MPXV. Blood was collected within 2 minutes of virus administration in order. These samples were used to confirm successful delivery ensuring proper infection and resulting disease. Following challenge, peripheral blood and oropharyngeal swabs were collected according to the schedule provided in Figure 1. Anesthetized physical examinations, including weights, rectal temperatures, and lesion assessments, were performed at the time of blood collection (Figure 1). Meloxicam was administered daily after the onset of lesions and continued until resolution of disease. Animals were provided subcutaneous lactated ringers solution whenever signs of dehydration (e.g., skin tenting, changes in mucous membranes) were present. Following infection, cage-side observations were performed at least once daily and increased to at least twice daily when animals began to demonstrate clinical signs (changes in responsiveness, appearance of lesions, etc.). Euthanasia criteria was based on a combination of responsiveness and prostration, as well as temperature. Animals were humanely euthanized under deep anesthesia via cardiac administration of a pentobarbital-based euthanasia solution whenever they became moribund, or at the designated end-of-study (Day 26 post-challenge).

Infectious viral titrations

Sample (cell culture stocks/inoculum, whole blood, and swabs) preparation and plaque titrations for cell culture material were carried out as previously described using Vero E6 cell monolayers in 6-well plates.⁶⁰ Briefly, after freeze thaw and sonication of sample, 10-fold dilutions were made in modified Eagle's medium (MEM) containing 2% heat inactivated fetal bovine serum (FBS) (stocks/inoculum), MEM containing 2% heat inactivated FBS and antimycotic/antibiotics (swabs), or 1X PBS with no magnesium or calcium and antimycotic/antibiotics (whole blood). A volume of 0.1 mL was added to wells and adsorbed for approximately 1 h before a liquid overlay was applied. For whole blood samples, wells were washed with 1X PBS (no magnesium or calcium) after adsorption.

Quantitation of MPXV nucleic acid

Total nucleic acid was extracted from whole blood for viral load quantification. Briefly, 100 μl whole blood was mixed with 100 μl buffer ATL (Qiagen), incubated at 56°C for 15 min at 300 RPM in a shaker incubator, and extracted using the Qiagen 1&2 Virus Mini Kit 2.0. Samples were eluted in 90 μl elution buffer. A standard curve ranging from 5.6×10^5 – 5.6×10^1 PFU/ml was generated using the challenge stock virus extracted as described above. Extracted nucleic acid was serially diluted 1:10 and run on each real-time PCR plate. Five μl extracted nucleic acid was tested by real-time PCR using the TaqPath 1-Step RTqPCR Master Mix, CG (ThermoFisher Scientific) according to the manufacturer's instructions using the primers MPOX-F3L-F290, MPOX-F3L-R396a, and probe MPOX-F3L-p333. Cycling conditions on the QuantStudio Dx (ThermoFisher Scientific) were: $25^{\circ}\text{C} \times 2$ min; $50^{\circ}\text{C} \times 15$ min; $95^{\circ}\text{C} \times 2$ min; 45 cycles ($95^{\circ}\text{C} \times 3$ sec, $60^{\circ}\text{C} \times 30$ sec). A sample was considered negative if the Cq value was below 40 cycles.

Luminex assay

Recombinantly expressed antigens from VACV (A27L, A33R, B5R, and L1R), MPXV (A29L, A35R, and B6R), and VARV antigens (A31, A36, B7, and M1) were produced as previously described.²⁰ Antigens were coupled to Magplex fluorescently bar-coded beads (Luminex) utilizing carboxyl chemistry via sulfo-N-hydroxysulfosuccinimide and 1-Ethyl-3-[3-dimethylaminopropyl]carbodiimide hydrochloride (Thermo Fisher) per the manufacturer's instructions. Coupled beads were incubated with inactivated NHP serum samples,

after dilution and heat inactivation, for 2 h at 37°C, with gentle shaking. Samples were incubated with beads at previously optimized dilutions to detect total IgG (1:50,000), IgG1 (1:10,000), IgG2a (1:10,000), IgG2b (1:2,500), IgG3 (1:1,000), IgA (1:1,000), and Fc γ Rs: Fc γ R2b (1:10,000), and Fc γ R3 (1:10,000). Each sample was assayed in technical duplicate. Beads were washed to remove any unbound sample and incubated with phycoerythrin (PE)-labeled secondaries. Anti-Ig isotypes were run at 0.65 μ g/mL (Southern Biotechnology, 6200-09; NHP Reagent Resource AB_2819304, AB_2819311, AB_2895608, AB_2895616, AB_2819323). For all anti-Ig reagents except anti-IgG, reagent was washed off and Streptavidin-PE was added at 1 μ g/mL and incubated 30 minutes RT with shaking. Recombinant biotinylated Fc gamma receptors were utilized at 1 μ g/mL (Sino Biological) and formed into tetramers using Streptavidin-PE at a 4:1 molar ratio and incubated 10 minutes. A molar excess of biotin was spiked in and incubated 10 minutes. The resulting tetramers were added to the wells. Excess detection antibody was removed through washing and samples were analyzed on Flexmap 3D (Luminex).

MAGPIX and recombinant antigens

Recombinantly expressed antigens from VACV (A27L, A33R, B5R, and L1R) and MPXV (A29L, A35R, and B6R) were produced as previously described.^{14,15,19} Magnetic microspheres and xMAP antibody coupling kits were purchased from Luminex Inc. (Austin, TX, USA). Phosphate buffered saline, Tween-20, skim milk powder, and goat α -human IgG (H&L) phycoerythrin conjugate (α -human-PE, 1 mg/mL) was produced using the PE lightning link kit (Abcam) as per the manufacturer's instructions after antibody was purchased from Sigma-Aldrich (St. Louis, MO, USA).

Antigens were covalently linked to microspheres following manufacturer instructions. For all steps that required removal of the solution, microspheres were immobilized by placing a rare-earth magnet adjacent to the reaction vessel, and the solution was removed by pipet. Whenever possible, microspheres were protected from light with aluminum foil. Briefly, 12.5 million microspheres were washed three times with 500 μ L of activation buffer and resuspended in 274.5 μ L of activation buffer. Next, 144.0 μ L of sulfo-N-hydroxysulfosuccinimide and 81.5 μ L of 1-ethyl-3-(3-dimethylaminopropyl) carbodiimide hydrochloride solutions were added and tubes were gently rotated for 20 min. After activation, microspheres were washed three times with coupling buffer and antigen was added at 4 μ g per million microspheres. The reaction was allowed to incubate for 2 h, after which the microspheres were washed three times with 500 μ L of PBS-T (PBS with 0.05% Tween-20), resuspended at 12.5 million microspheres per mL in PBS-T, and stored at 4°C. To allow for multiplexed assays, each antigen was coupled to distinct microspheres: VACV A27L on #45, VACV A33R on #75, VACV B5R on #78, MPXV A29L on #22, MPXV A35R on #12, and MPXV B6R on #19.

Relative antibody presence was determined by titration of sera on the Magpix® platform using 96-well plates. Sera was diluted 1:100 in 5% skim milk in PBS-T followed by 5-fold serial dilution to a final dilution of 1:7.8 x 10⁶. Samples were incubated with microspheres for 1 h; 50 μ L of sample and 2500 microspheres of each antigen per well. After incubation, microspheres in each well were washed three times with 100 μ L of PBS-T. Goat α -human-PE was diluted 1:100 in 5% skim milk in PBS-T, applied to microspheres at 50 μ L per well, and allowed to incubate for 1 h. Microspheres were washed three times with PBS-T, suspended in 100 μ L of PBS-T, and read by the Magpix® instrument. Samples were run in duplicate, and each plate included positive and negative control sera. Antibody titers were determined as the dilution factor at which signal divided by negative control signal dropped to 10.

Lysed MVA ELISA

Purified MVA was inactivated by water bath sonication for 3 min. ELISA plates (Millipore Sigma, M9410) were coated with 4 μ g/mL diluted MVA and incubated at 4°C overnight. Plates were washed 4x with 1x PBS-T before blocking at 37°C for 1 hr with SuperBlock (Thermo Scientific, 37580). NHP sera was heat inactivated at 56°C for 30 min prior to use in assay. Sera was diluted in assay buffer (PBS-T + 5% goat serum) before adding 75 μ L to respective wells and incubating for 1 hr at 37°C. After washing as above, HRP-linked goat anti-NHP (Invitrogen, Cat # PA1-84631; 1:500) was added and plates were incubated at 37°C for 1 hr. After washing, plates were incubated with 100 μ L TMB (Sera Care, Cat # 5120-0075) for 10 min followed by the addition of 100 μ L TMB Stop Solution (Sera Care, Cat # 5150-0020). Plate OD values were read at 450 nm. All data were analyzed using GraphPad Prism Software.

PRNT for the MV form of poxviruses

MV neutralization assays were performed as previously described.⁶¹ Briefly, dilutions of heat inactivated serum or anti-L1 antibody were incubated with MPXV clade I or IIA at a target of 100 PFU/well (e.g., 2000 PFU/mL) for approximately 1 h. The samples were then plaque titrated, stained with crystal violet and plaques enumerated. The PRNT50 titer was reported as the reciprocal of the highest dilution where virus (plaque number) was reduced by 50% relative to a negative control. Samples exhibiting less than 50% were assigned a titer of 14.1, equating to our lowest final dilution (1:20) divided by the square root of two. This is a common method for ascribing a value to samples below the limit of the assay.

PRNT for the EV form of poxviruses

EV neutralization assays were performed similarly to those reported.¹⁶ Briefly, HEK 293T and Vero 76 cells were infected with the Western Reserve strain of vaccinia virus at an MOI of 0.5, incubated for 48 h and supernatants collected and clarified via

centrifugation. The resultant supernatants were plaque titrated in the presence of anti-MV antibody (Mab-7D11) and human complement. To determine the content of released cell-associated virus versus total EV, monoclonal antibodies c6C and c8A were used as controls.⁵² Titer determinations and the assignment of values for specimens with activity below the assay limit are the same as defined for MV neutralization.

GFP-expressing VACV and MPXV neutralization

A semi-automated, flow cytometric neutralization assay was carried out using VACV strain WR or MPXV Z-79 expressing *Aequorea coerulescens* green fluorescent protein as previously described.⁵⁵ Two-fold dilutions of heat-inactivated serum (56°C for 30 min) from individual animals were prepared in 96-well, round bottom polypropylene plates using spinner modified minimum essential medium containing 2% fetal bovine serum. Approximately 2.5×10^4 PFU of VACV-WR or MPXV-Z-79 GFP expressing viruses were added to each well and plates incubated at 37°C for 1 h. After incubation, 10^5 HeLa S3 cells were pipetted into each well and plates were incubated for an additional 16 to 18 h at 37°C. The cells were fixed in 2% paraformaldehyde and GFP expression quantitated using a FACS Canto II flow cytometer and FlowJo software (BD Biosciences). NT50 values were calculated using Prism software (GraphPad/Dotmatics). The LOD was determined for sera obtained from mock-immunized animals by removing outlier NT50 values and calculating 1.65 x standard deviation. Procedures with infectious MPXV were performed in a registered Select Agent BSL-3 laboratory by trained and smallpox vaccinated investigators using protocols approved by the NIH Institutional Biosafety Committee.

Antibody-dependent complement deposition

Antibody-dependent complement deposition (ADCD) was performed similarly as described previously.⁶² Antigens were coupled to Luminex Magplex beads and immune complexes were formed as described above in the Multiplex Luminex Assay. Plates were washed, and guinea pig complement (Cedarlane) (diluted in 1x PBS with calcium and magnesium) was added to plates. Plates were incubated at 37°C, shaking at 700 rpm, for 20 min. Plates were washed with 15 μ M EDTA in PBS, and Fluorescein-conjugated goat IgG anti-guinea pig complement C3 detection antibody (MP Biomedicals #MP0855385) was added. Fluorescence was acquired on an Intelliflex (Luminex), and data are reported as the median fluorescence intensity (MFI). Assays were run in duplicate, and the data reflects the average of duplicates.

Antibody-dependent cellular phagocytosis

Antibody-dependent cellular phagocytosis (ADCP) was performed as described previously.²⁰ Briefly, antigen was biotinylated and coupled to FluoSpheres NeutrAvidin-Labeled Microspheres, 1.0 μ m, yellow-green (Invitrogen). Immune complexes were formed by mixing antigen-coupled beads with diluted serum and incubated for 2 h at 37°C. After incubation, THP-1 cells (ATCC) were added at a concentration of 1.25×10^5 cells/well, and plates were incubated for 18 h at 37°C. After overnight incubation, cells were fixed with 4% paraformaldehyde (PFA). Fluorescence was acquired on an iQue3 (Sartorius). A phagosome was calculated as: (%bead+ THP1 * GeoMean bead+ cells)/100000.

Antibody-dependent neutrophil phagocytosis

Antibody-dependent neutrophil phagocytosis (ADNP) was performed as described previously.⁶³ White blood cells were isolated from fresh, peripheral whole blood from healthy donors (Research Blood Components). All donors were above 18 years old, gave informed consent and were deidentified. White blood cells were isolated by ammonium-chloride-potassium (ACK) lysis. Antigen was biotinylated and coupled to FluoSpheres NeutrAvidin-Labeled Microspheres, 1.0 μ m, yellow-green (Invitrogen). Immune complexes were formed by mixing antigen-coupled beads with diluted serum and incubated for 2 h at 37°C. After incubation, Neutrophils were added at a concentration of 2.5×10^5 cells/well, and plates were incubated for 1 h at 37°C. Neutrophils were stained by anti-CD66b PacBlue (Biolegend 305112). Cells were fixed with 4% paraformaldehyde (PFA). Fluorescence was acquired on an iQue3 (Sartorius). A phagosome was calculated as: (%bead+ neutrophil * GeoMean bead+ neutrophils)/100000.

Antibody-dependent NK cell activation

Antibody-dependent NK cell activation (ADNKA) was performed as described previously.⁶⁴ NK cells were enriched from buffy coats via negative selection using RosetteSep (StemCell Technologies) and a Ficoll gradient was used to isolate NK cells. Buffy coats were obtained from BioIVT from healthy, screened donors. NK cells were rested overnight in RPMI with 10% Fetal Bovine Serum (FBS) and 2 ng/mL IL-15 at 37°C, 5% CO₂. ELISA plates were coated with antigen, blocked with 5% BSA, and sera diluted to a previously determined dilution was added and incubated overnight at 4°C. The following day, plates were washed, and NK cells were added to the plates at a concentration of 5×10^4 cells/mL in media with Brefeldin A (Sigma), Golgistop (BD Biosciences), and anti-CD107a BV605 (Biolegend, Clone H4A3, cat 328634). Plates were incubated for 5 h at 37°C, 5% CO₂. After incubation, cells were stained for surface markers with anti-CD56 APC (Biolegend, clone MEM-188, cat 304610) and anti- CD3 APC-Cy7 (Biolegend, clone UCHT1, cat 300426). Cells were fixed and permeabilized with Fixation Medium A and B (Invitrogen) and stained with anti-MIP1b-BV421 (BD Biosciences, clone D21-1351, cat 562900) and anti-IFN γ -PE (Biolegend, clone B27, cat 506507). Fluorescence was acquired on an iQue3 (Sartorius). NK cells were gated as CD56+/CD3- and activity was determined as the percent of NK cells that were positive for CD107a, IFN- γ , or MIP-1b.

QUANTIFICATION AND STATISTICAL ANALYSIS

Unsupervised clustering of vaccine signature

The data for Principal component analyses (PCA) was logarithmized and z-scored first. PCA clustered the data points (animals) projected on the first two principal components (PCs). The PCs were generated via high-dimensional reduction of overall antibody features, in which each PC represents a linear combination of the features and remains orthogonal to other PCs but retains as much of the variance in the feature dataset as possible. The degree to which each feature contributed to the orthonormal principal component coefficients was also calculated. Principal Component Analysis was performed using R `prcomp` function.

Correlates analyses

The minimal antibody correlates of vaccine outcomes were identified using a supervised machine-learning approach- Least Absolute Shrinkage and Selection Operator (LASSO), followed by partial least-squares regression analysis (PLSR). The data was logarithmized and z-scored first. Then LASSO was performed in a repeated cross-validation framework and the features identified in more than 60% repeated models were set as selected features. After feature selection, PLSR was used to define the relationship between the input as a linear combination of the selected features and the vaccine outcome (viral load or number of lesions). Specifically, PLSR seeks the latent variables, which linearly combine the features, which explain the maximum variance of the outcome. Model interpretation and predictive ability metrics were assessed using sum of squares for the variation, and variation in the outcome that can be predicted, and the square root of mean error estimate. To estimate the statistical significance of the final model, a permutation test were performed to shuffle the outcome labels across the samples. The randomly shuffled dataset was then used to test the likelihood of obtaining a model prediction accuracy by chance. Each permutation test was performed 10,000 times to generate an empirical null distribution and an exact p value. A p value of less than 0.001 between actual and both permutation tests resulted in the rejection of the null hypothesis, and was considered statistically significant, providing confidence in the robustness of the model and the identified correlates. Analyses were performed with R version 4.3.0 (2023-04-21). LASSO was performed using `glmnet` R package version 4.1.4. Partial Least Squares Regression (PLSR) and model diagnostics was performed using `ropls` R package version 1.30.0.

Correlation network analysis

The correlation network, which interrogates correlations among LASSO-PLSR model-selected correlates and other antibody features, may provide further mechanistic understanding in antibody-related immunity. To do this, the network was constructed based on the Spearman correlation coefficients (ρ) between any paired individual features. Only the correlations with Benjamini-Hochberg -adjusted $p < 0.01$ and absolute $\rho > 0.7$ will be remained in the correlation network.

Supplemental figures

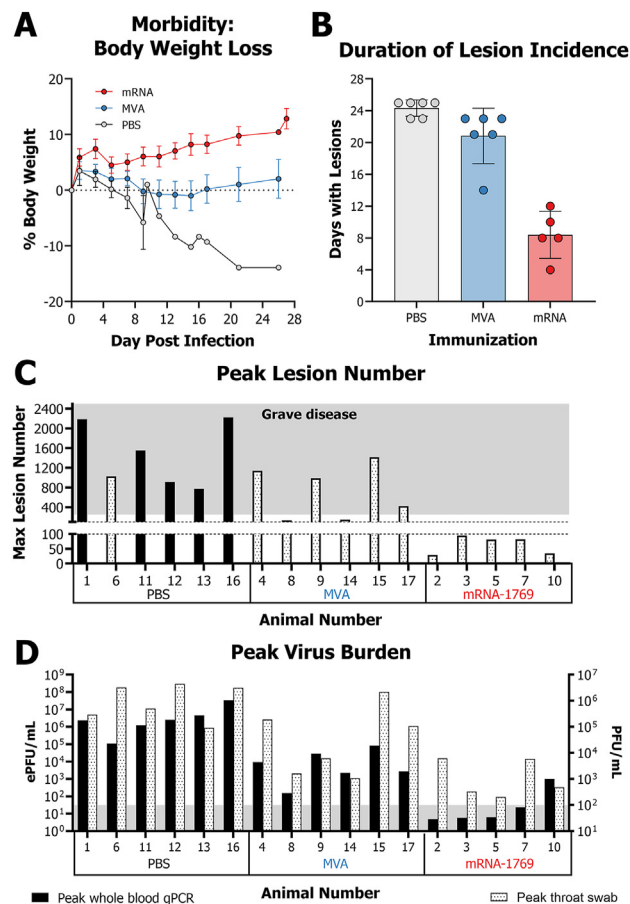


Figure S1. Observational data after mpox virus challenge in the NHP model, related to Figure 1

(A) Body weight was observed per animal during the course of infection. Percent body weight change is reported as the average \pm SEM for each group ($n = 5-6$ /group).

(B) The duration of lesion incidence is reported for each individual animal, with the bar representing the average \pm SEM for each group ($n = 5-6$ /group). Control (PBS) immunized animals that succumbed to infection were reported as non-resolving the lesions for the course of the challenge.

(C) The maximum lesion number per animal noted during the course of disease is reported. Severe disease is denoted as greater than 100 lesions per animal, while grave disease is considered to be greater than 250 lesions per animal.

(D) Maximum virus burden during the challenge course was measured by quantitative PCR for whole blood or plaque assay for throat swabs. The gray shaded area represents the lower limit of detection for the plaque assay.

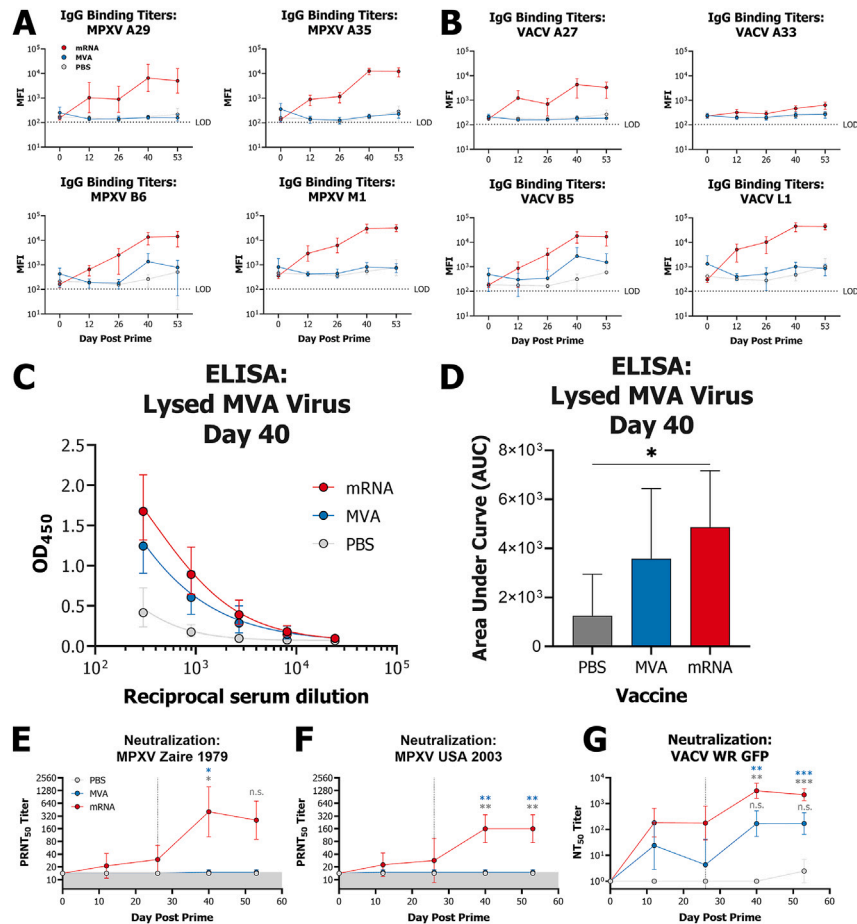


Figure S2. Immunological measurements as IgG binding titers per individual antigen, to whole, lysed MVA virions, or neutralization, related to Figure 2

(A and B) Antibody binding titers were determined via a multiplex Luminex assay for all (A) MPXV and (B) VACV-derived recombinant proteins at all serological time points pre-infection. Geometric mean titers \pm geometric SD are shown for each group ($n = 6/\text{group}$). Limit of detection (LOD) for the assay is denoted as a dashed line.

(C–F) Antibody binding titers were determined using an ELISA with whole, lysed MVA as coating reagent for serum collected at day 40 post-prime. (C) Raw binding curves or (D) area under curve values are shown for each group ($n = 6/\text{group}$). Antibody titers were determined via plaque reduction neutralization test for MPXV strains (E) clade I Zaire 1979 and (F) clade 2 USA 2003 at all serological time points pre-infection. (E and F) Limit of detection (LOD) for the assay is denoted as a shaded box.

(G) A GFP-reporter vaccinia virus strain Western Reserve was used to determine neutralization titers through reduction of GFP-positive cells. Geometric mean titers \pm geometric SD are shown for each group ($n = 6/\text{group}$). One-way ANOVA with Tukey's correction for multiple comparisons ($*p < 0.05$, $**p < 0.01$, $***p < 0.001$, and $****p < 0.0001$).

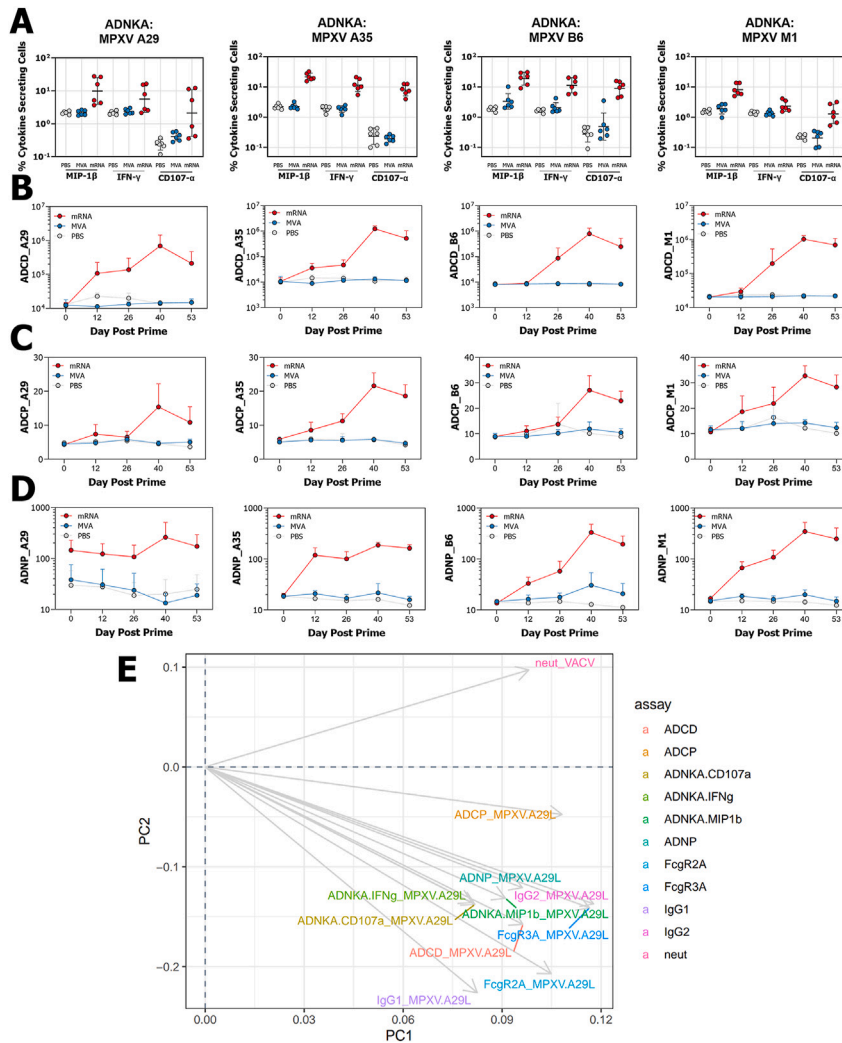


Figure S3. Fc-functional antibody effector responses at pre-challenge time points, related to Figure 3

(A) Antibody-dependent NK cell activation was performed using sera from animals taken two weeks post boost and assayed for secretion of CD107a, IFN γ , and MCP1 β cytokines. Percent cytokine-secreting cells is reported for each antigen and each cytokine.

(B–D) Antibody-dependent complement deposition, (C) antibody-dependent cell-mediated phagocytosis, or (D) neutrophil phagocytosis were assayed using sera for time points collected pre-challenge.

(E) Loadings of the measurements included in principal-component analysis (Figure 3F) were visualized.

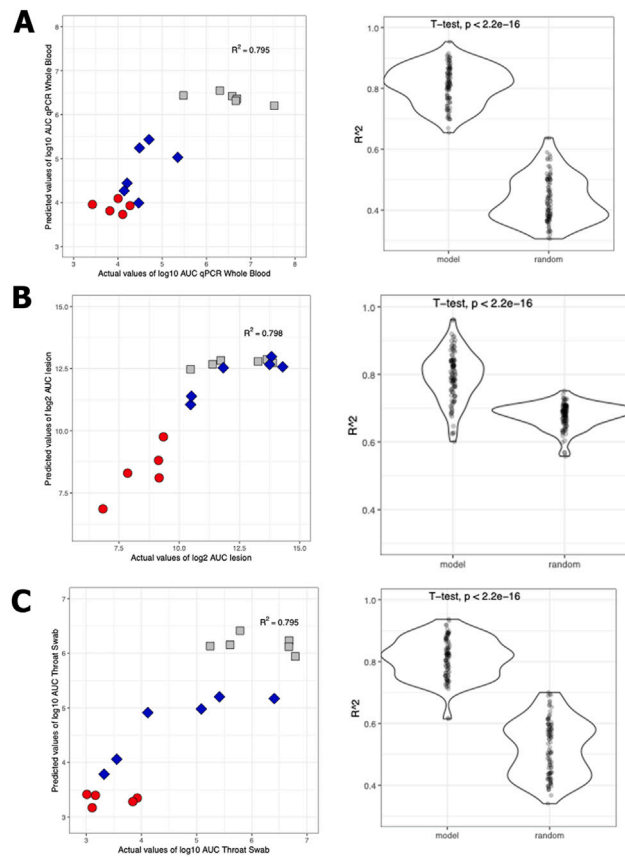


Figure S4. Significance diagnostics of PLSR models, related to Figure 4

For PLSR models shown in Figure 4A, the predicted outcome values were compared with the actual outcome values. R^2 were calculated 100 times by sampling 10 random samples out of 17 using the selected features (model violin). This is then compared with R^2 of randomly selected feature models, where the same size of feature set was used but selected randomly.